Supplementary Materials

"Oncohistone Mutations Occur at Functional Sites of Regulatory ADP-ribosylation"

Huang *et al.* (2022)

This document contains the following: Page

1) Supplementary Table 4

- Supplementary Table S1. Top 20 somatic missense mutations in oncohistones. 4

2) Supplementary Figures 5

- Supplementary Fig. S1. Identification of histone ADPRylation sites on native nucleosomes isolated from MCF-7 cells by mass spectrometry 5
- Supplementary Fig. S2. Proliferation of MCF-7 cells expressing prevalent oncohistone D/E mutants 6
- Supplementary Fig. S3. Proliferation of OVCAR-3 cells expressing prevalent oncohistone D/E mutants 8
- Supplementary Fig. S4. Proliferation of MDA-MB-231 cells expressing prevalent oncohistone D/E mutants 10
- Supplementary Fig. S5. Sites of growth-regulating oncohistone D/E mutations mapped onto the nucleosome structure 11
- Supplementary Fig. S6. Mutation of the H2B-D51 ADPRylation site does not affect the proliferation of normal cells 12
- Supplementary Fig. S7. H2B-D51 mutants exhibit reduced levels of PARylation in MDA-MB-231 cells: Longer exposure of the Western blot 13
- Supplementary Fig. S8. Mutation of the H4-D68 ADPRylation site enhances cell proliferation in MDA-MB-231 cells 14
- Supplementary Fig. S9. H2B-D51 mutants increase H2B acetylation, but not H3K27 acetylation 15
- Supplementary Fig. S10. p300-mediated H2BK12ac levels increase in MDA-MB-231 cells ectopically expressing H2B-D51 mutants and are blocked by A485 16
- Supplementary Fig. S11. H2B-D51 oncohistone mutants promote genome-wide H2BK12 acetylation 17
- Supplementary Fig. S12. Distance between altered ATAC-seq peaks and the TSSs of regulated genes 18
- Supplementary Fig. S13. H2B-D51 oncohistone mutations link site-specific histone ADPRylation, chromatin accessibility, H2BK12 acetylation, and gene expression outcomes 19

- Supplementary Fig. S14. Relationship between PARP-1, p300, and H2BK12ac enrichment at specific gene regions in MDA-MB-231 cells 21
- Supplementary Fig. S15. The H2B-D51N ADPRylation site mutant alters chromatin accessibility to facilitate the binding of specific TFs....22
- Supplementary Fig. S16. Genomic analysis of the enrichment of histone PTMs at ATAC-seq peaks altered by the H2B-D51N ADPRylation site mutant 23
- Supplementary Fig. S17. Western blot analyses of protein expression in MDA-MB-231 xenograft tumors 24
- Supplementary Fig. S18. H4-D68 ADPRylation site mutants promote the accumulation of γH2AX foci in MDA-MB-231 cells....25
- Supplementary Fig. S19. H4-D68 ADPRylation site mutants promote the accumulation of γH2AX foci in MDA-MB-468 cells....26

3) Supplementary Data Set 27

- Supplementary Data Set 1. Mass spectrometry data for identification of histone ADPRylation sites in MCF-7 cells 27
- Supplementary Data Set 2. Mass spectrometry data for identification of histone PTM sites in MDA-MB-231 cells expressing H2B mutants 27

4) Supplementary Materials and Methods 28

- Cell culture....28
- Cell treatments 28
- Antibodies....28
- Generation of lentiviral expression vectors for wild-type and site mutant histones....28
- Generation of stable ectopic protein expression cell lines....29
- Cell proliferation assays....29
- Cell migration assays 29
- Preparation of cell extracts and Western blotting....29
  - *Preparation of whole cell lysates....29*
  - *Preparation of cell fractions....30*
  - *Determination of protein concentrations and Western blotting 30*
- Nucleosome immunoprecipitation....30
- Identification of histone PTMs by mass spectrometry 31
  - *Processing of native nucleosomes isolated from MCF-7 cells for identification of histone ADPRylation sites....31*
  - *Processing of nucleosomes isolated from MDA-MB-231 cells expressing FLAG-tagged wild-type or mutant histone H2B for identification of histone PTMs....31*
  - *Identification of histone PTMs by mass spectrometry....31*
- Expression and purification of recombinant proteins 32
  - *Purification of PARP-1 expressed in Sf9 insect cells 32*
  - *Purification of p300 expressed in Sf9 insect cells 32*
  - *Purification of histone H2B expressed in E. coli....33*
  - *Purification of NMNAT-1 expressed in E. coli....33*

- In vitro PARylation assays....34
- In vitro HAT assays....34
- RNA-sequencing and data analysis....34
  - *Generation and sequencing of RNA-seq libraries....34*
  - *Analysis of RNA-seq data....35*
  - *Gene ontology (GO) analyses....35*
- ATAC- sequencing and data analysis....35
  - *Generation and sequencing of ATAC-seq libraries....35*
  - *Analysis of ATAC-seq data....35*
- Crosslinked chromatin immunoprecipitation (ChIP) and ChIP-qPCR....36
  - *Crosslinked chromatin immunoprecipitation....36*
  - *ChIP-qPCR....36*
- Native ChIP and ChIP-sequencing....37
  - *Native chromatin immunoprecipitation....37*
  - *ChIP-seq library preparation....37*
  - *Analysis of ChIP-seq data....37*
- Integration, analysis, and visualization of ChIP-seq, ATAC-seq, and RNA-seq data....38
- Immunofluorescent staining and confocal microscopy....38
- Cell-derived xenograft experiments in mice....39
- Quantification and statistical analysis....39

5) Supplementary References....40

1) Supplementary Table

Supplementary Table S1. Top 20 somatic missense mutations in oncohistones.
Related to Fig. 1.

	Histone			
Mutations (Rank Order)	**H2A**	**H2B**	**H3**	**H4**
1	S1C	E76K	E97K	R3C
2	E121Q	F70L	K36M	S1C
3	E121K	E113K	K27M	L49F
4	R29Q	E113Q	E105K	K79N
5	R17P	E71Q	R131C	G4D
6	K75N	E2Q	G34R	E52Q
7	K74N	P103S	D81N	R92T
8	E56Q	E93D	E73K	R45Q
9	S1L	E76Q	E105Q	G4S
10	G37D	E2K	K4M	G28V
11	E92D	S14F	R83C	E63Q
12	E121D	S123N	R2G	E53D
13	R11C	R99C	G34V	D68Y
14	Q104H	Q47E	E73Q	D68N
15	N73K	K27N	E133Q	D68H
16	N38K	G104W	R134T	A89T
17	L34F	E35K	Q5H	E53K
18	H31Y	E35D	E50D	D85N
19	E92K	D68N	D123H	A15V
20	E61D	D51N	D106N	A15T
Number (Percent) of D/E mutations	**7 (35%)**	**12 (60%)**	**10 (50%)**	**8 (40%)**
Number of Unique Mutation Sites	**15**	**16**	**17**	**15**
Number of Unique D/E Mutation Sites	**4**	**8**	**8**	**5**

The data in this table were extracted from Nacev *et al.* (2019). The 80 mutations total across the four core histones represent 63 unique sites of mutation, with 25 (40%) of them occurring at Glu or Asp residues.

2) Supplementary Figures

A

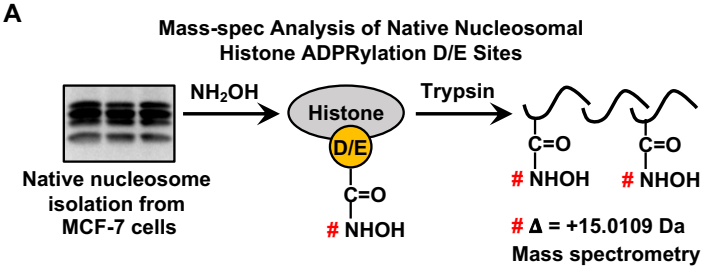

B

D/E ADPRylation Sites Identified by Mass Spectrometry				
Histone	**Amino Acid**			
H2A	E56	D90	E91	E92
H2B	D2*	E2*	D51	E71
H3	E94	E97	E105	
H4	D24	D85		

* H2B-D2 was identified on H2B variant H2BC18, H2BC9, and H2BU1, while H2B-E2 was identified on H2BS1.

Supplementary Fig. S1. Identification of histone ADPRylation sites on native nucleosomes isolated from MCF-7 cells by mass spectrometry.
A) Schematic representation of the process used to identify Glu/Asp ADPRylation sites on native nucleosomes isolated from MCF-7 cells. ADPRylation sites were identified after treatment of the isolated nucleosomes with hydroxylamine, which reduced the complexity of the ADPR modification, creating an adduct on Glu and Asp residues that was readily identifiable by a predictable +15.0109 Da shift using mass spectrometry.
B) Table includes the Glu/Asp ADPRylation sites identified on core histones in at least one out of four replicates. This screen was not saturated and not all the ADPRylation sites were identified. The asterisk (*) indicates that H2B-D2 was identified on H2B variants H2BC18, H2BC9, and H2BU1, while H2B-E2 was identified on H2B variant H2BS1.
Related to Fig. 1.

Supplementary Fig. S2 is on the next page.

Supplementary Fig. S2. Proliferation of MCF-7 cells expressing prevalent oncohistone D/E mutants.

A) Growth of MCF-7 cells ectopically expressing FLAG-tagged wild-type (WT), E2A, E35A, D51A, D68A, E71A, E76A, E93A, or E113A H2B was assayed by crystal violet staining. Each point represents the mean ± SEM, n = 4. Asterisks indicate significant differences between the mutant and WT at day 7 (two-way ANOVA followed by Dunnett's multiple comparisons test; **** $p < 0.0001$).

B) Growth of MCF-7 cells ectopically expressing FLAG-tagged WT, E50A, E73A, D81A, D97A, E105A, D106A, E123A, or E133A H3 was assayed by crystal violet staining. Each point represents the mean ± SEM, n = 4. Asterisks indicate significant differences between the mutant and WT at day 7 (two-way ANOVA followed by Dunnett's multiple comparisons test; * $p < 0.05$, and *** $p < 0.001$).

C) Growth of MCF-7 cells ectopically expressing FLAG-tagged WT, E52A, E53A, E63A, D68A, or D85A H4 was assayed by crystal violet staining. Each point represents the mean ± SEM, n = 3. Asterisks indicate significant differences between the mutant and WT at day 7 (two-way ANOVA followed by Dunnett's multiple comparisons test; ** $p < 0.01$).

D) Growth of MCF-7 cells ectopically expressing FLAG-tagged WT, E56A, E61A, E92A, or E121A H2A was assayed by crystal violet staining. Each point represents the mean ± SEM, n = 6.

E) Western blots showing ectopically-expressed FLAG-tagged WT and oncohistone mutants in MCF-7 cells.

Related to Fig. 1.

Supplementary Fig. S2.

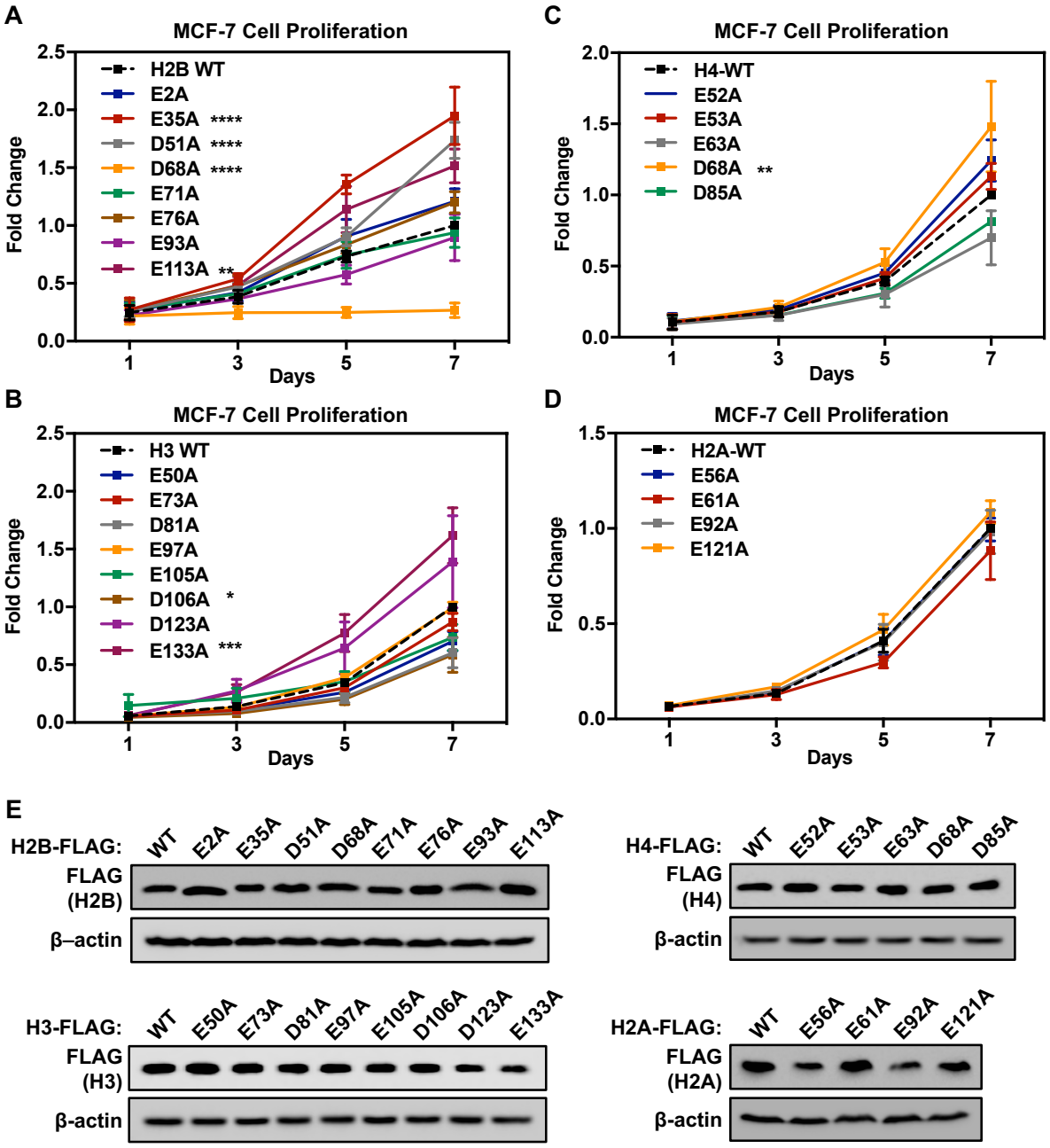

Supplementary Fig. S3 is on the next page.

Supplementary Fig. S3. Proliferation of OVCAR-3 cells expressing prevalent oncohistone D/E mutants.
A) Growth of OVCAR-3 cells ectopically expressing FLAG-tagged WT, E2A, E35A, D51A, D68A, E71A, E76A, E93A, or E113A H2B was assayed by crystal violet staining. Each point represents the mean ± SEM, n = 4. Asterisks indicate significant differences between the mutant and WT at day 7 (two-way ANOVA followed by Dunnett's multiple comparisons test; * $p < 0.05$).
B) Growth of OVCAR-3 cells ectopically expressing FLAG-tagged WT, E50A, E73A, D81A, D97A, E105A, D106A, E123A, or E133A H3 was assayed by crystal violet staining. Each point represents the mean ± SEM, n = 3. Asterisks indicate significant differences between the mutant and WT at day 7 (two-way ANOVA followed by Dunnett's multiple comparisons test; ** $p < 0.01$).
C) Growth of OVCAR-3 cells ectopically expressing FLAG-tagged WT, E52A, E53A, E63A, D68A, or D85A H4 was assayed by crystal violet staining. Each point represents the mean ± SEM, n = 3. Asterisks indicate significant differences between the mutant and WT at day 7 (two-way ANOVA followed by Dunnett's multiple comparisons test; * $p < 0.05$, and **** $p < 0.0001$).
D) Growth of OVCAR-3 cells ectopically expressing FLAG-tagged WT, E56A, E61A, E92A, or E121A H2A was assayed by crystal violet staining. Each point represents the mean ± SEM, n = 5.
E) Western blots showing ectopically-expressed FLAG-tagged WT and oncohistone mutants in OVCAR-3 cells.
Related to Fig. 1.

Supplementary Fig. S3.

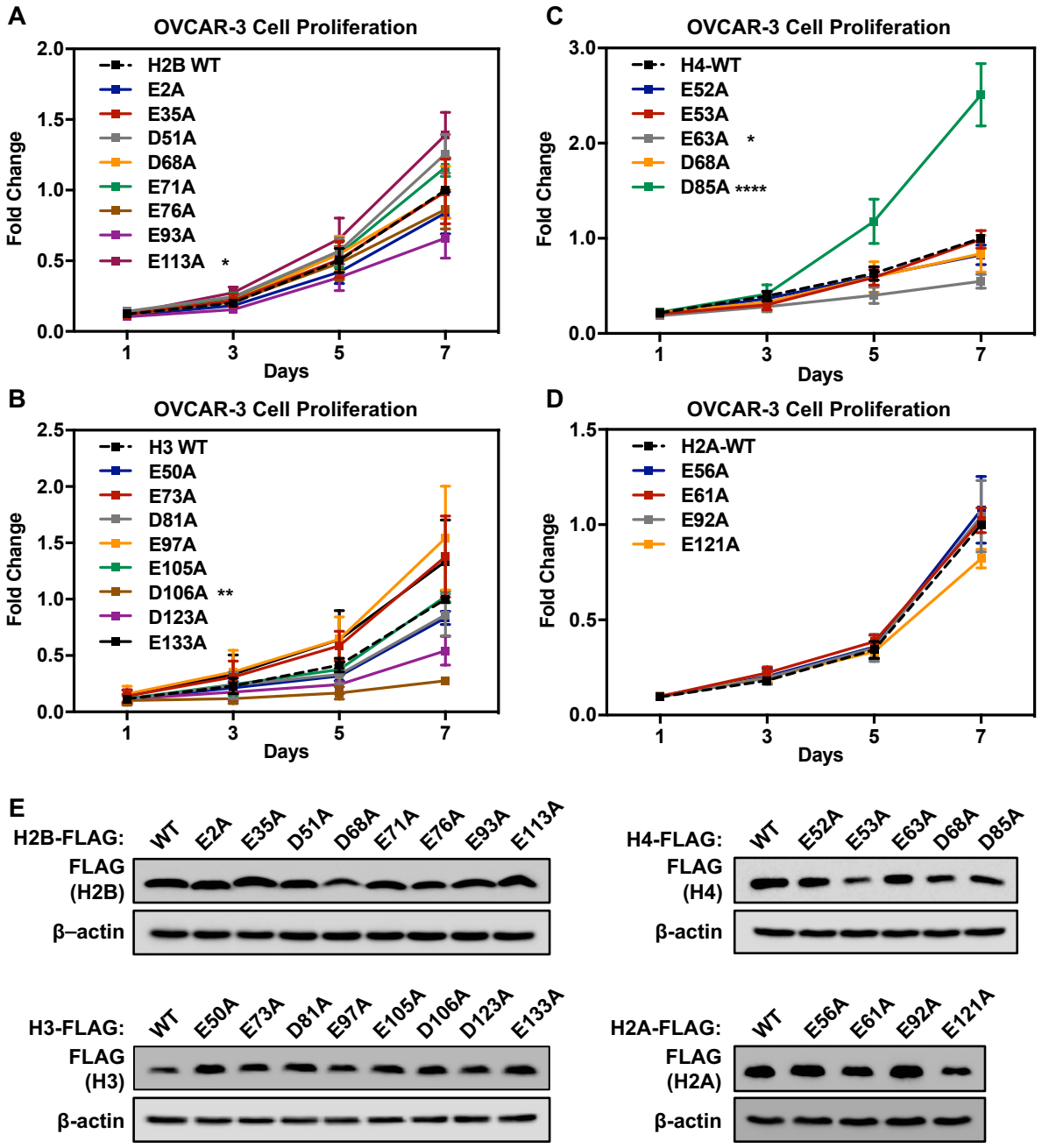

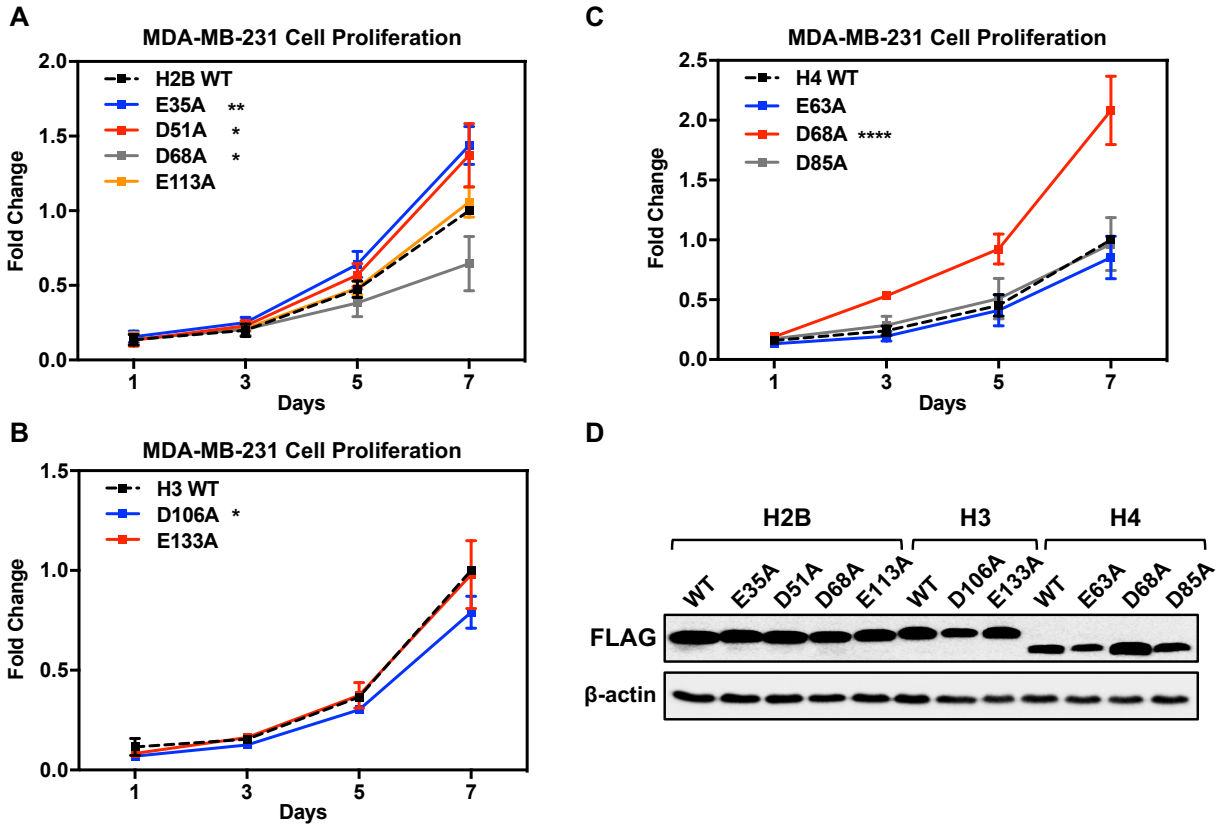

Supplementary Fig. S4. Proliferation of MDA-MB-231 cells expressing prevalent oncohistone D/E mutants.

A) Growth of MDA-MB-231 cells ectopically expressing FLAG-tagged WT, E35A, D51A, D68A, or E113A H2B was assayed by crystal violet staining. Each point represents the mean ± SEM, n = 5. Asterisks indicate significant differences between the mutant and WT at day 7 (two-way ANOVA followed by Dunnett's multiple comparisons test; * $p < 0.05$, ** $p < 0.01$).

B) Growth of MDA-MB-231 cells ectopically expressing FLAG-tagged WT, D106A, or E133A H3 was assayed by crystal violet staining. Each point represents the mean ± SEM, n = 4. Asterisks indicate significant differences between the mutant and WT at day 7 (two-way ANOVA followed by Dunnett's multiple comparisons test; * $p < 0.05$).

C) Growth of MDA-MB-231 cells ectopically expressing FLAG-tagged WT, E63A, D68A, or D85A H4 was assayed by crystal violet staining. Each point represents the mean ± SEM, n = 3. Asterisks indicate significant differences between the mutant and WT at day 7 (two-way ANOVA followed by Dunnett's multiple comparisons test; **** $p < 0.0001$).

D) Western blots showing ectopically-expressed FLAG-tagged WT and oncohistone mutants in MDA-MB-231 cells.

Related to Fig. 1.

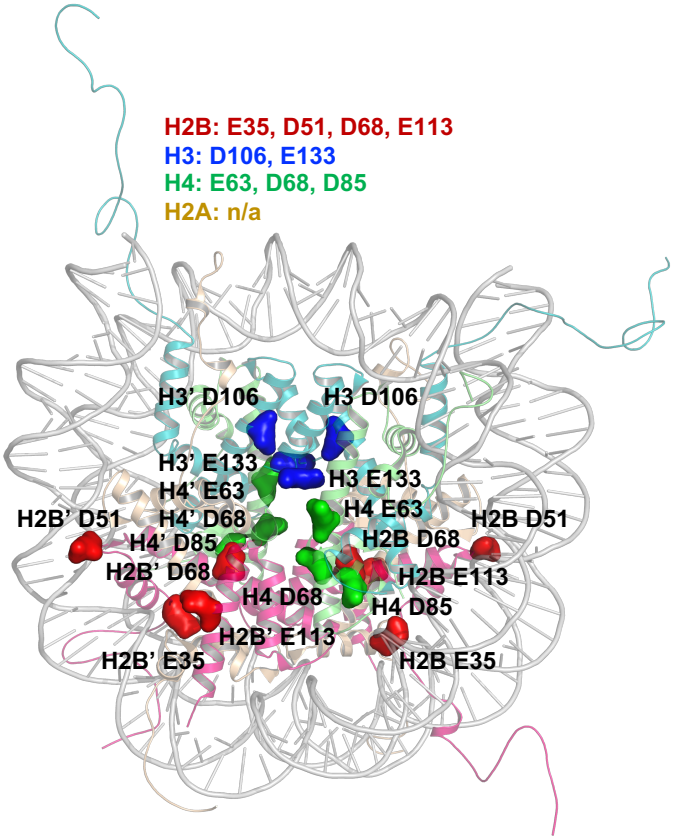

Supplementary Fig. S5. Sites of growth-regulating oncohistone D/E mutations mapped onto the nucleosome structure.
As summarized in Fig. 1D, the following oncohistone mutants alter the growth of two or three cancer cell lines when ectopically expressed in the cells - H2B: E35, D51, D68, E113; H3: D106, E133; H4: E63, D68, D85. In the figure, these D/E mutation sites are mapped onto the structure of the nucleosome. H2B is shown in red, H3 is shown in blue, H4 is shown in green, and H2A is shown in gold.
Related to Fig. 1.

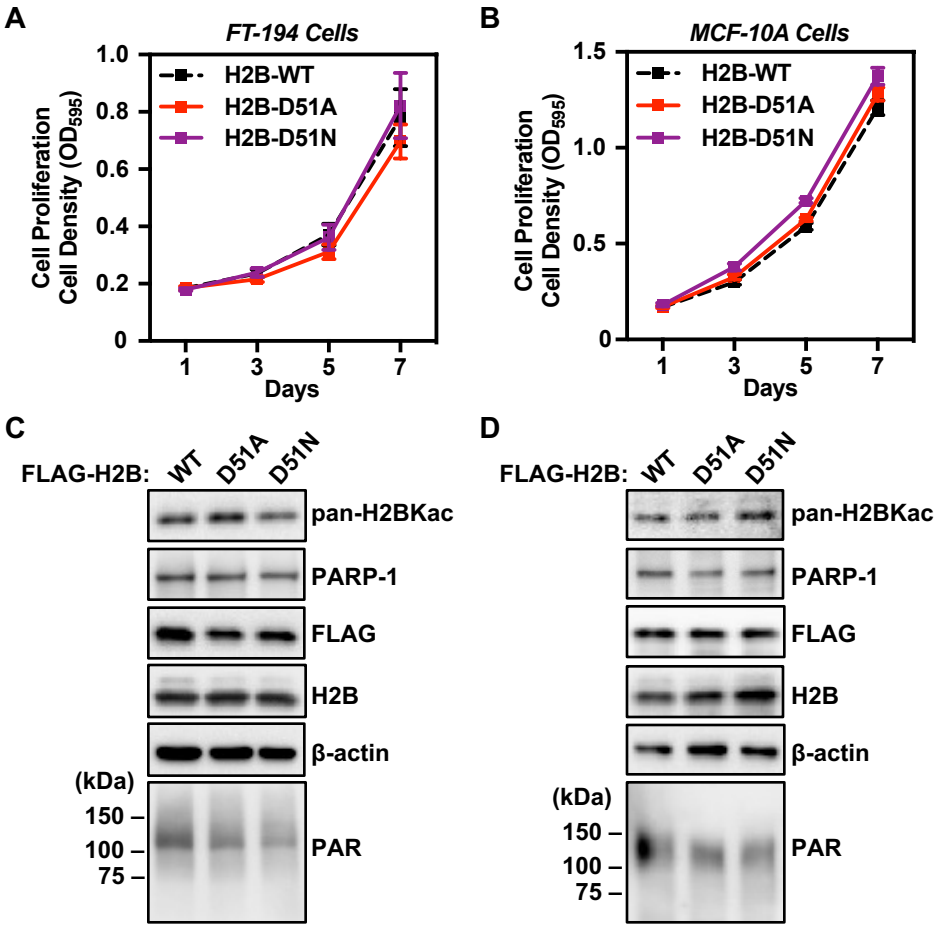

Supplementary Fig. S6. Mutation of the H2B-D51 ADPRylation site does not affect the proliferation of normal cells.

A and B) Growth curves of two "normal" cell lines: FT-194 (a normal fallopian tube cell line representing a suspected source of ovarian cancer progenitors) and MCF-10A (which is commonly used to represent normal mammary epithelial cells) ectopically expressing FLAG-tagged WT, D51A, or D51N H2B. Proliferation was assayed by crystal violet staining

C and D) Western blots showing the levels of pan-H2BKac, PARP-1, FLAG, H2B, and PAR in FT-194 and MCF-10A cells ectopically expressing FLAG-tagged WT, D51A, or D51N H2B. β-actin was used as a loading control.

Related to Fig. 2.

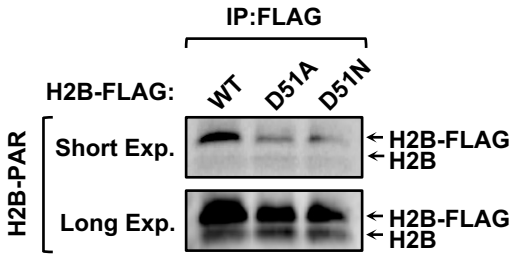

The short exposure is shown in Figure 2C

Supplementary Fig. S7. H2B-D51 mutants exhibit reduced levels of PARylation in MDA-MB-231 cells: Longer exposure of the Western blot.
Short exposure (also shown in Fig. 2C) and long exposure of Western blots showing the levels of ADPRylation on H2B in MDA-MB-231 cells ectopically expressing FLAG-tagged WT, D51A, or D51N H2B after immunoprecipitation of FLAG-tagged nucleosomes. The long exposure shows that endogenous H2B is also PARylated, but only ectopically expressed mutants show reduced PARylation.
Related to Fig. 2.

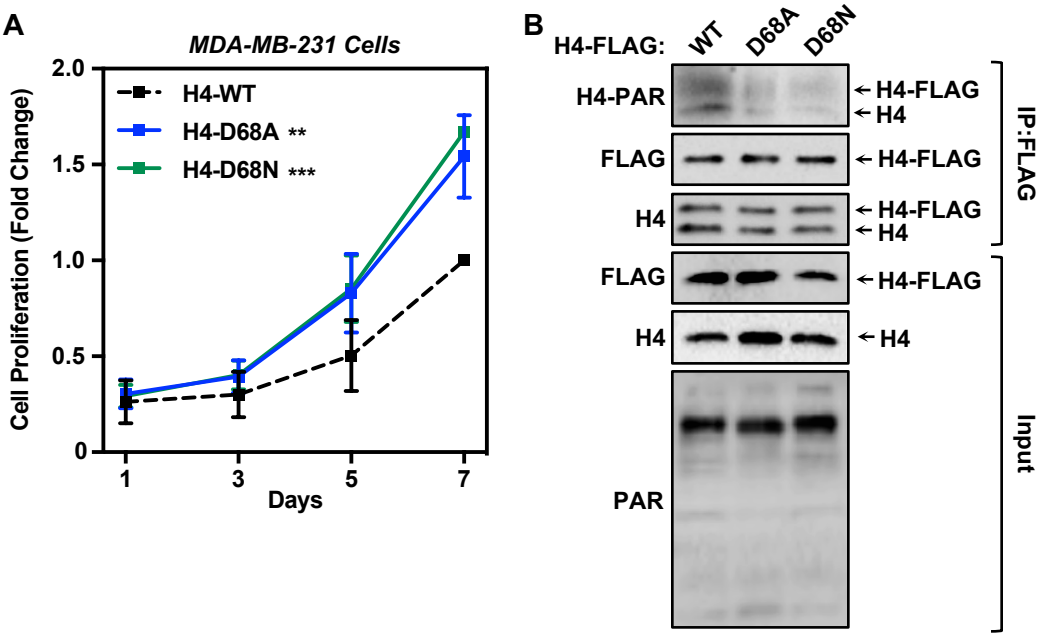

Supplementary Fig. S8. Mutation of the H4-D68 ADPRylation site enhances cell proliferation in MDA-MB-231 cells.

A) Growth curves of MDA-MB-231 cells ectopically expressing FLAG-tagged WT, D68A, or D68N H4 assayed by crystal violet staining. Each point represents the mean ± SEM, n = 3. Asterisks indicate significant differences between the mutant and WT at day 7 (two-way ANOVA followed by Dunnett's multiple comparisons test; * $p < 0.05$, and ** $p < 0.01$).

B) Western blots showing the levels of ADPRylation on H4 in MDA-MB-231 cells ectopically expressing FLAG-tagged WT, D68A, or D68N H4 after immunoprecipitation of FLAG-tagged nucleosomes.

Related to Fig. 2.

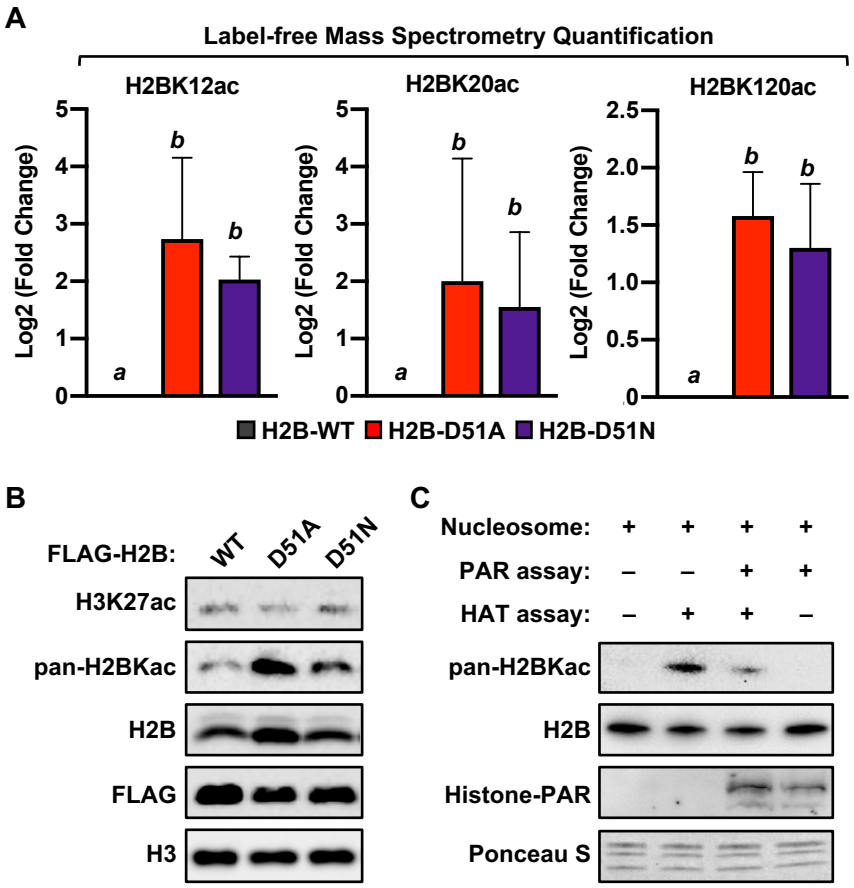

Supplementary Fig. S9. H2B-D51 mutants increase H2B acetylation, but not H3K27 acetylation.

A) Quantification of mass spectrometry results for H2BK12ac, H2BK20ac, and H2BK120ac in MDA-MB-231 cells expressing FLAG-tagged WT, D51A, or D51N H2B. The results represent Log_2 of the abundance of modified peptides (fold change of H2B D51 mutant versus H2B WT) for the individual histone modifications. Three biological replicates of FLAG-tagged nucleosomes isolated by immunoprecipitation from MDA-MB-231 cells were submitted for LC-MS/MS identification. Bars marked with different letters are significantly different from each other (one-way ANOVA followed by Dunnett's multiple comparisons test; $p < 0.01$).

B) Western blots showing that H3K27ac levels were not altered in MDA-MB-231 cells expressing FLAG-tagged WT, D51A, or D51N H2B.

C) In vitro PARylation assays were performed using recombinant human mononucleosomes, PARP-1, NMNAT-1, NAD^+, ATP, and 25-mer DNA. The reactions were stopped by the addition of the PARP inhibitor PJ34, followed by HAT assays with the addition of p300 and acetyl-CoA. Western blots showing the levels of pan-H2BKac and histone-PAR. Blots for H2B and Ponceau S staining were used to assess equal loading of material.

Related to Fig. 3.

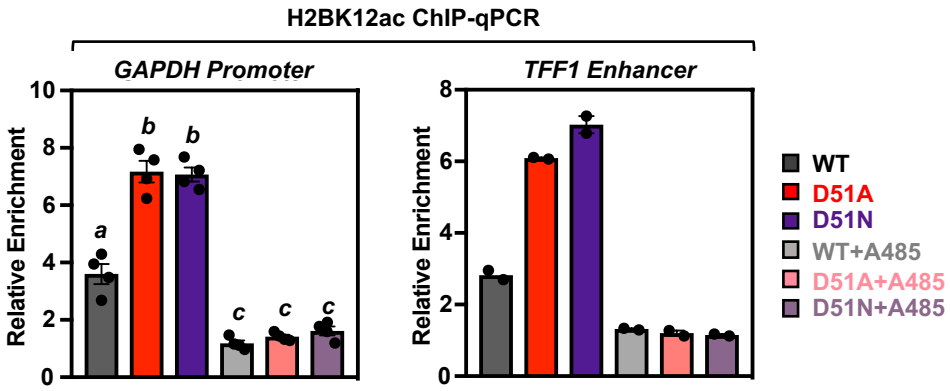

Supplementary Fig. S10. p300-mediated H2BK12ac levels increase in MDA-MB-231 cells ectopically expressing H2B-D51 mutants and are blocked by A485.
Native ChIP for H2BK12ac followed by qPCR assays in MDA-MB-231 cells ectopically expressing FLAG-tagged WT, D51A, or D51N H2B ± treatment with the p300 inhibitor A485 (5 μM, 2 hours) as indicated. H2BK12ac enrichment was assessed at the promoters of the *GAPDH* (n = 4) and *TFF1* (n = 2) genes using gene-specific primers. Bars marked with different letters are significantly different from each other (one-way ANOVA followed by Dunnett's multiple comparisons test; $p < 0.05$).
Related to Fig. 4.

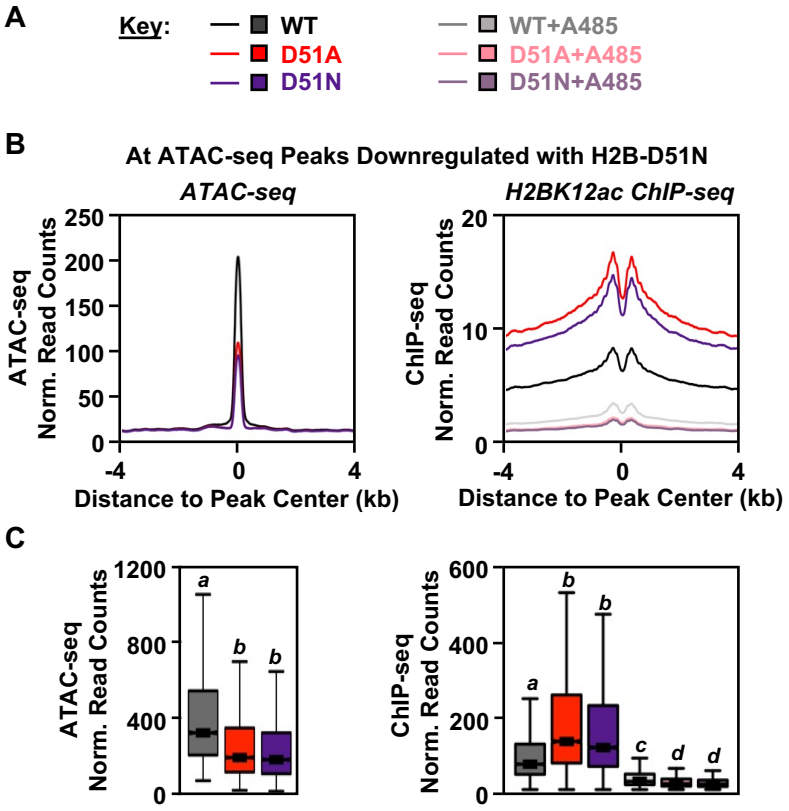

Supplementary Fig. S11. H2B-D51 oncohistone mutants promote genome-wide H2BK12 acetylation.

A) Key for the conditions used in the other panels of this figure. H2BK12ac ChIP-seq and ATAC-seq were performed in MDA-MB-231 cells ectopically expressing FLAG-tagged WT, D51A, or D51N H2B ± treatment with A485 (5 μM, 2 hours) or vehicle (DMSO).

B and C) Metaplots (B) and box plots (C) of ATAC-seq (*left*) and H2BK12ac ChIP-seq (*right*) data at ATAC-seq peaks downregulated in cells expressing the H2B-D51N oncohistone mutant versus cells expressing WT H2B. Bars marked with different letters are significantly different from each other (Wilcoxon rank sum test, $p < 1 \times 10^{-13}$).

Related to Fig. 4.

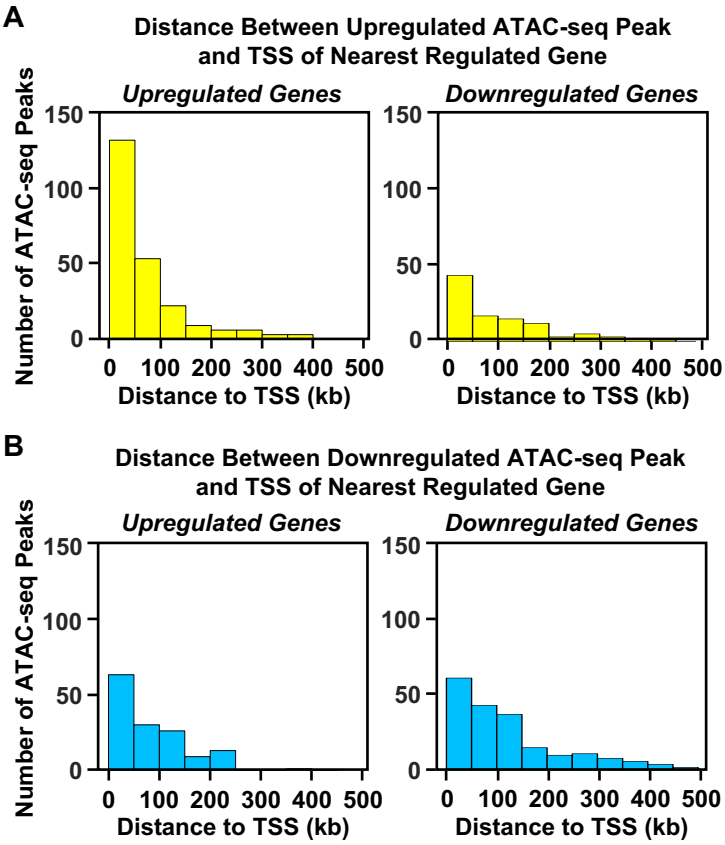

Supplementary Fig. S12. Distance between altered ATAC-seq peaks and the TSSs of regulated genes.
As shown in Fig. 5, chromatin accessibility (i.e., ATAC-seq) and gene expression (i.e., RNA-seq) that was up- or downregulated by expression of the H2B-D51N mutant (versus WT H2B) in MDA-MB-231 cells, was used to categorize ATAC-seq peaks into four groups: ATAC-seq peaks upregulated (Group A) or downregulated (Group B) with the H2B-D51N mutant located nearest to an upregulated gene, and ATAC-seq peaks upregulated (Group C) or downregulated (Group D) with the H2B-D51N mutant located nearest to a downregulated gene.
A and B) Histogram plots showing the number of upregulated (A) or downregulated (B) ATAC-seq peaks and their distance to the TSSs of the nearest gene upregulated (*left*) or downregulated (*right*) with the H2B-D51N mutant.
Related to Fig. 5.

Supplementary Fig. S2 is on the next page.

Supplementary Fig. S13. H2B-D51 oncohistone mutations link site-specific histone ADPRylation, chromatin accessibility, H2BK12 acetylation, and gene expression outcomes.
A and B) Metaplots (A) and box plots (B) of ATAC-seq (*left*) and H2BK12ac ChIP-seq (*right*) data at the Group D ATAC-seq peaks described in Fig. 5A (i.e., H2B-D51-downregulated ATAC-seq peaks located nearest to downregulated genes). Bars marked with different letters are significantly different from each other (Wilcoxon rank sum test, $p < 7 \times 10^{-5}$).
C and D) Metaplots (C) and box plots (D) of H2BK12ac ChIP-seq (*left*) and RNA-seq (*right*) data at the TSSs of downregulated genes nearest to the Group D ATAC-seq peaks described in Fig. 5A. Bars marked with different letters are significantly different from each other (Wilcoxon rank sum test, $p < 8 \times 10^{-7}$ for ChIP-seq data and $p < 9 \times 10^{-4}$ for RNA-seq data).
E) Key for the conditions used in the other panels of this figure. Genomic assays were performed in MDA-MB-231 cells ectopically expressing FLAG-tagged WT, D51A, or D51N H2B ± treatment with A485 (5 μM, 2 hours) or vehicle (DMSO).
F) Genome browser tracks representing the RNA-seq, ATAC-seq, and H2BK12ac ChIP-seq data at a genomic locus (*MMP3*) containing a gene downregulated upon expression of the H2B-D51 oncohistone mutants in MDA-MB-231 cells.
Related to Fig. 6.

Supplementary Fig. S13.

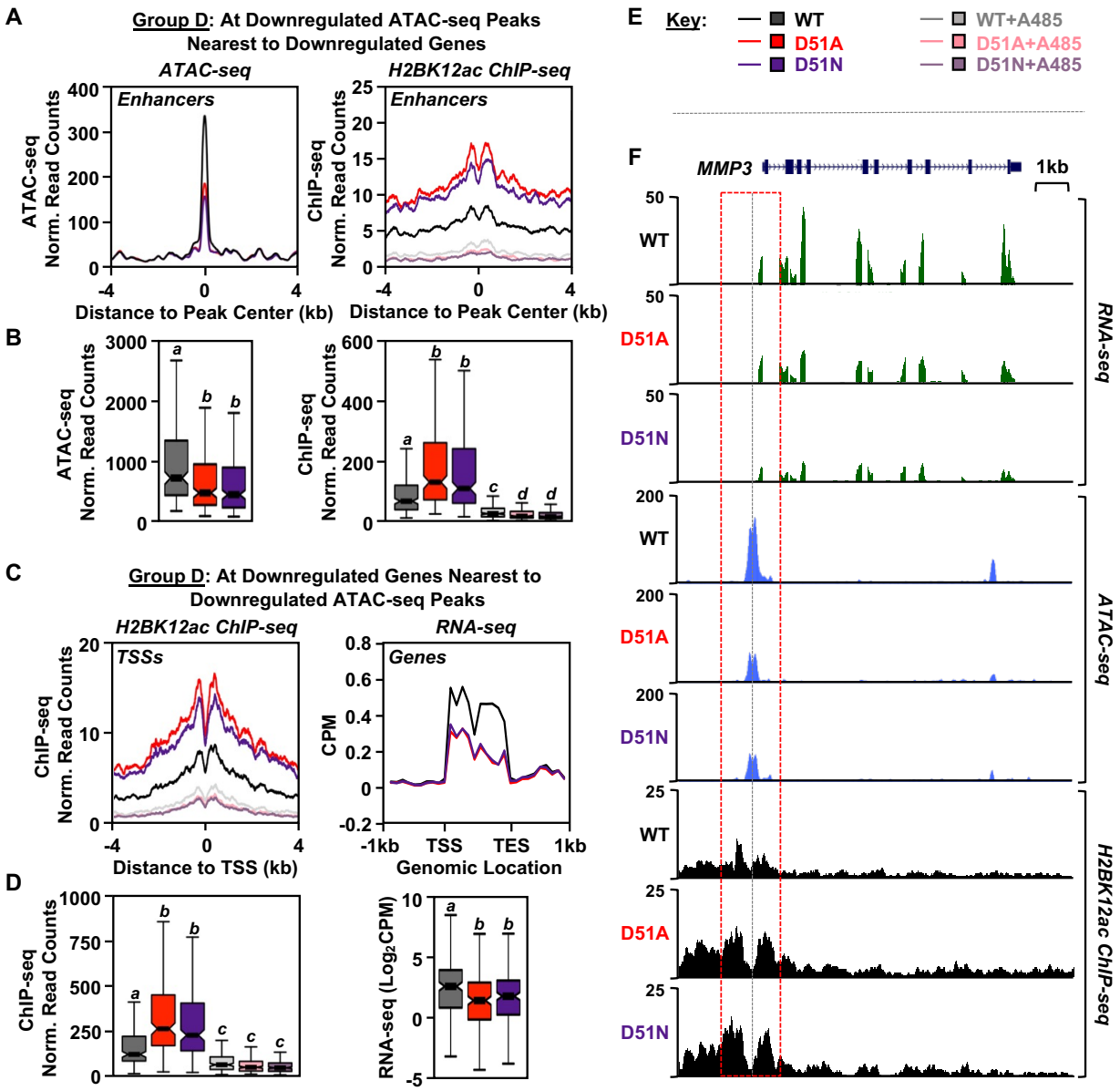

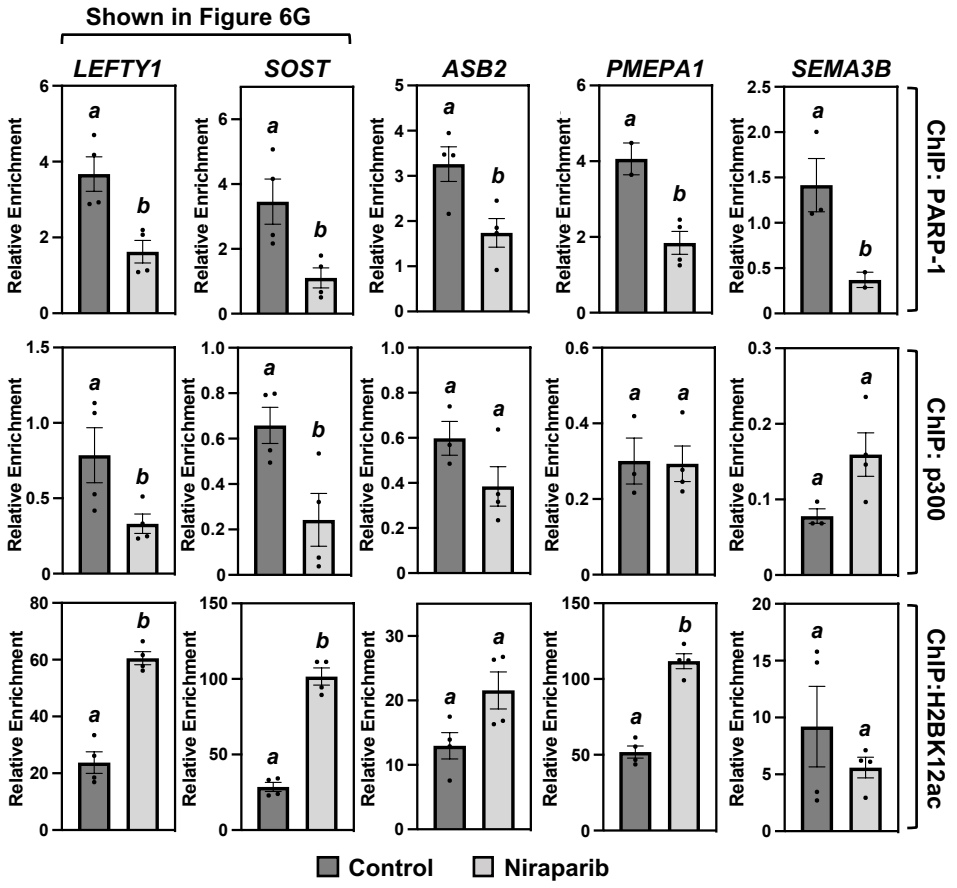

Supplementary Fig. S14. Relationship between PARP-1, p300, and H2BK12ac enrichment at specific gene regions in MDA-MB-231 cells.
ChIP-qPCR assays for PARP-1, p300, and H2BK12ac in MDA-MB-231 cells treated with vehicle or the PARP inhibitor Niraparib (10 μM, 2 hours) as indicated. PARP-1, p300, and H2BK12ac enrichment was assessed at the *LEFTY1* and *SOST* enhancers (also shown in Fig. 6G), as well as at the *ASB2*, *PMEPA1* and *SEMA3B* enhancers, using gene-specific primers. These sites exhibit increased acetylation of H2BK12 by ChIP-seq in the presence of the H2B-D51 ADPRylation site mutants. Each column represents the mean ± SEM (n = 4). Bars marked with different letters are significantly different from each other (Student's t-test; $p < 0.05$).
Related to Fig. 6.

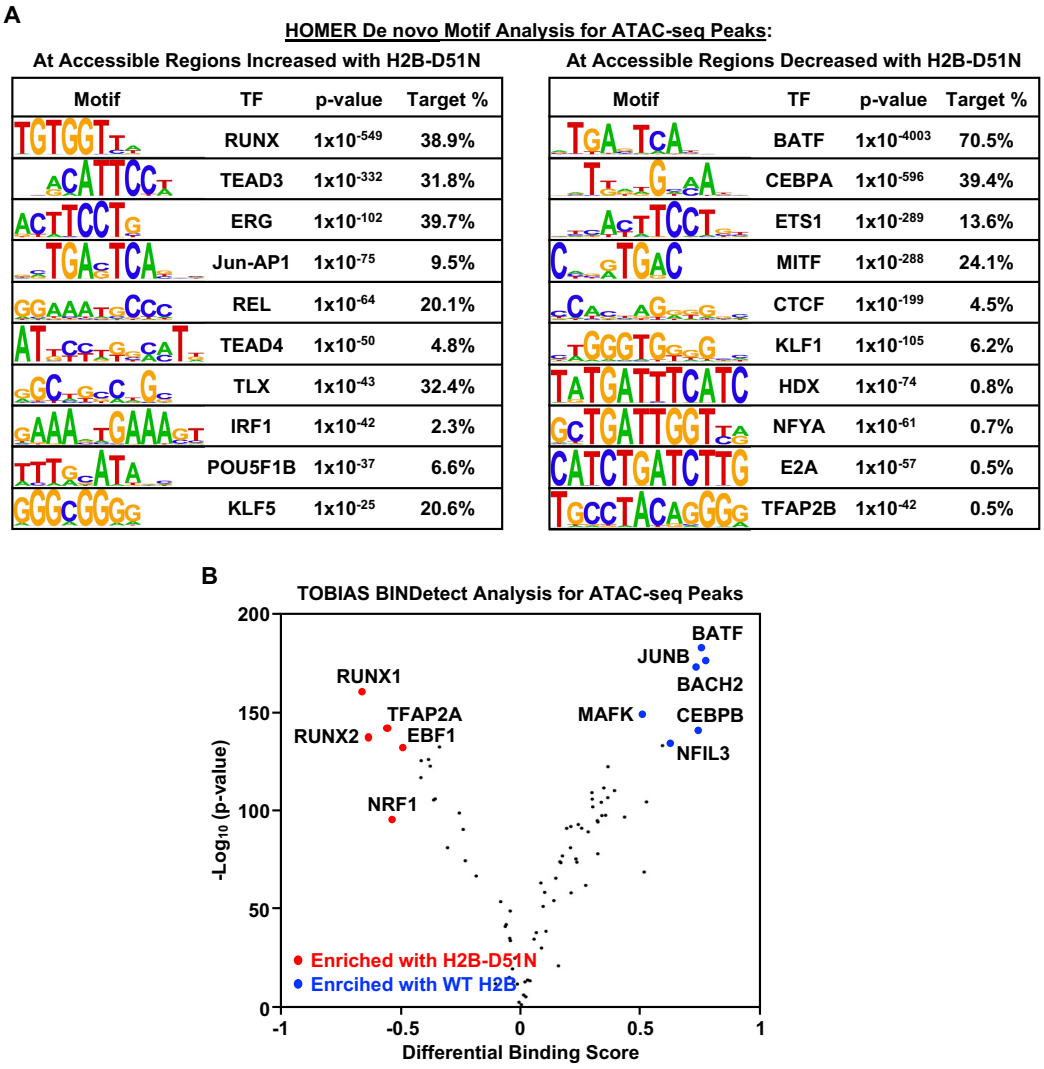

Supplementary Fig. S15. The H2B-D51N ADPRylation site mutant alters chromatin accessibility to facilitate the binding of specific TFs.

A) De novo motif analysis of ATAC-seq peaks at accessible chromatin regions altered with the H2B-D51N mutant compared to WT H2B. ATAC-seq peaks up- or downregulated with the H2B-D51N mutant (*left* and *right*, respectively) were used to identify TFs enriched in differentially accessible regions using HOMER. The motif sequence web logos, predicted TFs, p-values, and percent of targets (i.e., peaks) containing the motif are shown.

B) Volcano plot showing the differential binding scores and -$\log_{10}$ (p-values) for the TFs at accessible chromatin regions altered with the H2B-D51N mutant compared to WT H2B analyzed using TOBIAS where each dot represents a TF. Significantly enriched TF motifs with -$\log_{10}$ (p-value) above the 95% quantile or differential binding scores in the top 5% in each direction are colored and shown with labels. Significantly enriched TF motifs with higher binding scores in the presence of H2B-D51N are labeled in red and significantly enriched TF motifs with higher binding scores in the presence of WT H2B mutant are labeled in blue.

Related to Fig. 6.

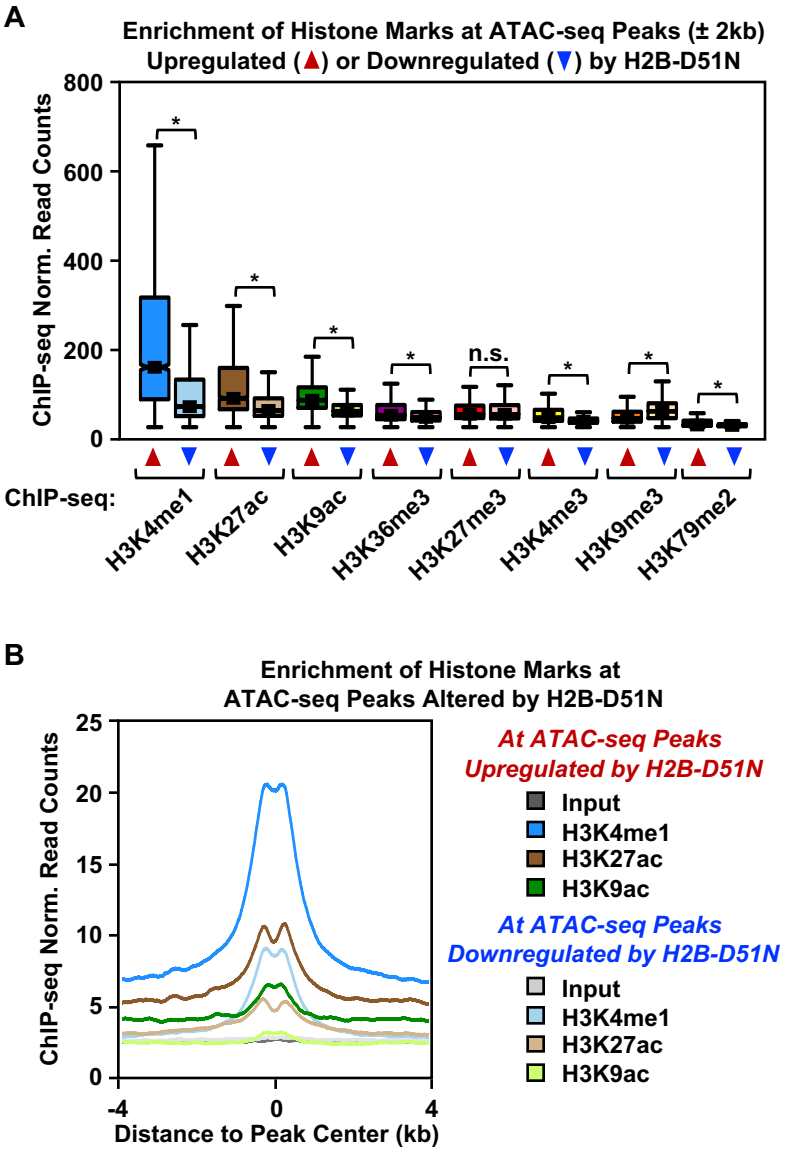

Supplementary Fig. S16. Genomic analysis of the enrichment of histone PTMs at ATAC-seq peaks altered by the H2B-D51N ADPRylation site mutant.

A) Genomic analysis of published ChIP-seq data (1) and our ATAC-seq data. The coordinates of ATAC-seq peaks altered by H2B-D51N were lifted over to hg19. ChIP-seq reads in ± 2 kb window around the ATAC-seq peak were calculated and normalized to sequencing depth to plot as boxplots using boxplot function in R. Wilcoxon rank sum tests were performed to determine the statistical significance between the two groups for each histone mark. Asterisks indicate significant differences as indicated (Wilcoxon rank sum test, $p < 2.2 \times 10^{-16}$).

B) Average ChIP-seq profiles of the top three histone PTMs as observed in the boxplots were plotted as metaplot using metaplot function in groHMM package of R.

Related to Fig. 6.

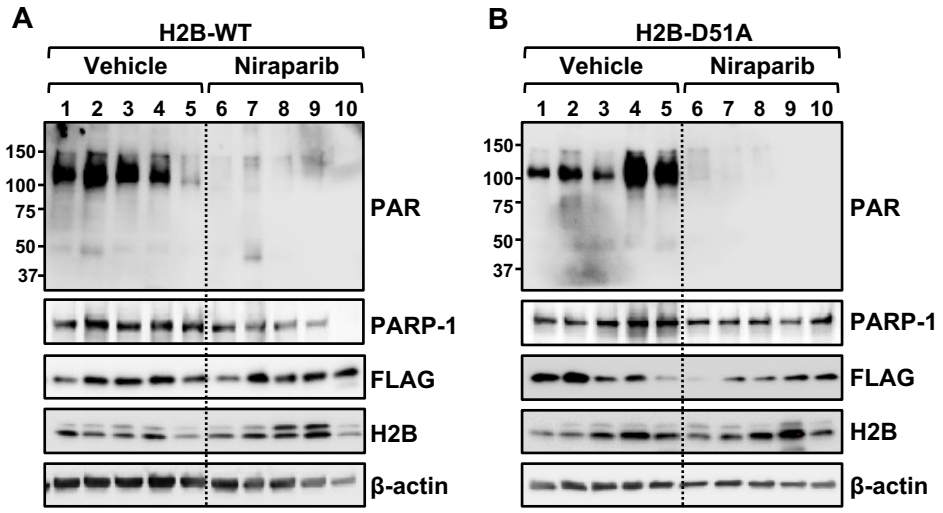

Supplementary Fig. S17. Western blot analyses of protein expression in MDA-MB-231 xenograft tumors.
Xenograft tumors were formed from MDA-MB-231 cells engineered for ectopic expression of FLAG-tagged H2B WT **(A)** or D51A mutant **(B)** in NOD *scid* gamma (NSG) mice, which were treated with vehicle or 25 mg/kg Niraparib intraperitoneally (i.p.) 5 days a week over 4 weeks. Whole tissue extracts were prepared from samples of the frozen tumor tissues and blotted for the proteins/epitopes indicated. Each lane represents a sample of one tumor collected from one mouse. *Related to Fig. 7.*

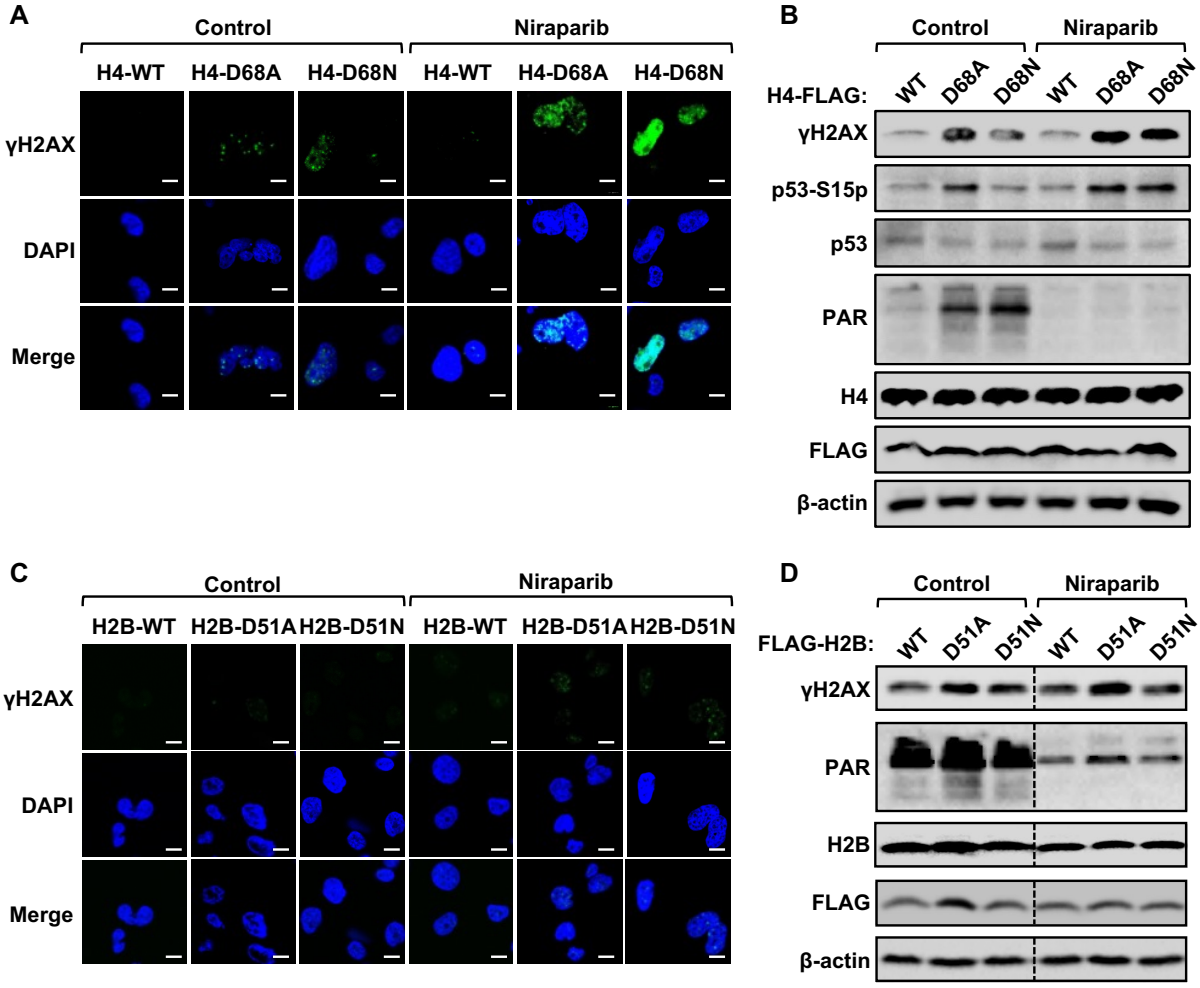

Supplementary Fig. S18. H4-D68 ADPRylation site mutants promote the accumulation of γH2AX foci in MDA-MB-231 cells.

A) Immunofluorescent staining of γH2AX in MDA-MB-231 cells expressing FLAG-tagged WT, D68A, or D68N H4 with Niraparib treatment or vehicle (DMSO). Scale bar = 10μm. The experiment was performed three times to ensure reproducibility.

B) Western blots showing the levels of γH2AX, p53-S15p, p53, and PAR in MDA-MB-231 cells expressing FLAG-tagged WT, D68A, or D68N H4 with Niraparib treatment or vehicle (DMSO).

C) Immunofluorescent staining of γH2AX in MDA-MB-231 cells expressing FLAG-tagged WT, D51A, or D51N H2B with Niraparib treatment or vehicle (DMSO). Scale bar = 10μm. The experiment was performed three times to ensure reproducibility.

D) Western blots showing the levels of γH2AX and PAR in MDA-MB-231 cells expressing FLAG-tagged WT, D51A, or D51N H2B with Niraparib treatment or vehicle (DMSO).

Related to Fig. 7.

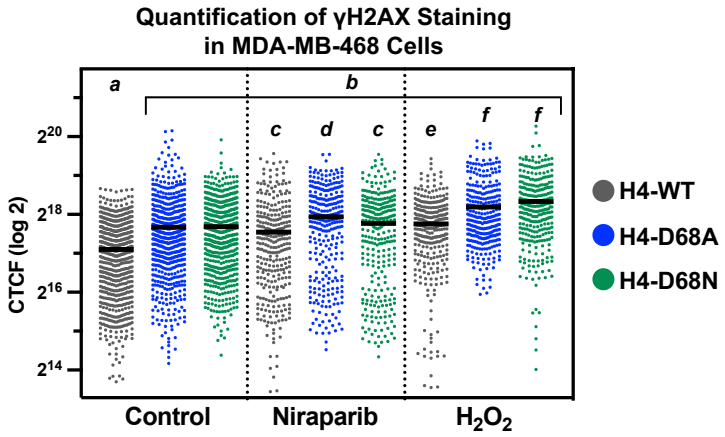

Supplementary Fig. S19. H4-D68 ADPRylation site mutants promote the accumulation of γH2AX foci in MDA-MB-468 cells.
Quantification of immunofluorescent staining of γH2AX in MDA-MB-468 cells expressing FLAG-tagged WT, D68A, or D68N H4, ± treatment with Niraparib, or H_2O_2. The signals in positively stained cells were quantified using ImageJ software and the corrected total cellular fluorescence (CTCF) values were plotted. The experiment was performed three times to ensure reproducibility. Bars marked with different letters are significantly different from each other (one-way ANOVA followed by Dunnett's multiple comparisons test; $p < 0.01$).
Related to Fig. 7.

3) Supplementary Data Set

Supplementary Data 1. Mass spectrometry data for identification of histone ADPRylation sites in MCF-7 cells.
Native nucleosomes were isolated from MCF-7 cells using micrococcal nuclease and incubated in 200 mM HEPES pH 8.8 in the presence of 0.75 M hydroxylamine (Sigma, 438227) at 4°C for 16 hours. The mononucleosomes were concentrated using centrifugal filter units (Millipore, UFC501024), and electrophoresed on a precast SDS-PAGE gel and visualized by Coomassie blue staining. Gel slices containing histone proteins were excised. The gel pieces were processed in UT Southwestern's Proteomics Core Facility and subjected to LC-MS/MS using an Orbitrap Fusion Lumos mass spectrometer. Raw MS data files were analyzed using Proteome Discoverer v2.2 (Thermo), with peptide identification performed using Sequest HT searching against the *Homo sapiens* database from UniProt. Fragment and precursor tolerances of 10 ppm and 0.6 Da were specified, and three missed cleavages were allowed. Carbamidomethylation of Cys was set as a fixed modification, with oxidation of Met set as a variable modification. For detection of ADPRylation sites, hydroxamic acid addition (+15.0109 Da) to Asp and Glu were set as variable modifications. The false-discovery rate (FDR) cutoff was 1% for all proteins and peptides.
See the separate Excel spreadsheet provided.
Related to Supplementary Fig. S1.

Supplementary Data 2. Mass spectrometry data for identification of histone PTM sites in MDA-MB-231 cells expressing H2B mutants.
Nucleosome immunoprecipitation was performed from MDA-MB-231 cells expressing FLAG-tagged wild-type or mutant histone H2B using anti-FLAG M2 agarose beads. The immunoprecipitated mononucleosomes were electrophoresed on a precast SDS-PAGE gel and visualized by Coomassie blue staining. Gel slices containing histone proteins were excised. The gel pieces were processed in UT Southwestern's Proteomics Core Facility and subjected to LC-MS/MS using an Orbitrap Fusion Lumos mass spectrometer. Raw MS data files were analyzed using Proteome Discoverer v2.2 (Thermo), with peptide identification performed using Sequest HT searching against the *Homo sapiens* database from UniProt. Fragment and precursor tolerances of 10 ppm and 0.6 Da were specified, and three missed cleavages were allowed. Carbamidomethylation of Cys was set as a fixed modification, and oxidation of Met, acetylation of Lys, mono, di, and trimethylation of Lys and Arg, phosphorylation of Ser, Thr, and Tyr, and ubiquitylation of Lys were set as variable modifications. The false-discovery rate (FDR) cutoff was 1% for all proteins and peptides.
See the separate Excel spreadsheet provided.
Related to Fig. 3.

4) Supplementary Materials and Methods

Cell culture

MCF-7, MDA-MB-231, OVCAR-3, MDA-MB-468, MCF-10A, FT-194, and 293T cells were purchased from the American Type Culture Collection. MCF-7 cells were maintained in Minimum Essential Medium Eagle (Sigma-Aldrich, M1018) supplemented with 5% bovine calf serum (Sigma-Aldrich, 12133C) and 1% penicillin/streptomycin. MDA-MB-231, OVCAR-3, and MDA-MB-468 cells were maintained in RPMI-1640 (Sigma-Aldrich, R8758) supplemented with 10% fetal bovine serum (Sigma-Aldrich, F8067) and 1% penicillin/streptomycin. MCF-10A cells were maintained in MEGM Mammary Epithelial Cell Growth Medium and supplement kit (Lonza, CC3150). FT-194 cells were maintained in DMEM/F12 (Corning, 15-090-CV) supplemented with 10% fetal bovine serum. 293T cells were cultured in DMEM (Cellgro, 10-017-CM) supplemented with 10% fetal bovine serum and 1% penicillin/streptomycin. Fresh cell stocks were regularly replenished from the original stocks, verified for cell type identity using the GenePrint 24 system (Promega, B1870), and confirmed as mycoplasma-free every three months using a commercial testing kit.

Cell treatments

Cells were grown until 70% confluence and treated for experiments described herein. The cells were treated with 5 μM A485 (Tocris Bioscience, 1104546-89-5), 5 to 20 μM Veliparib (Tocris Bioscience, 1104546-89-5), 2.5 μM, 5 μM, or 10 μM Niraparib (MedChemExpress, HY-10619), or DMSO vehicle for 2 hours.

Antibodies

The custom recombinant poly(ADP-ribose) binding reagent (anti-PAR) was generated and purified in-house (2) (now available from EMD Millipore; catalog no. MABE1031). The custom rabbit polyclonal antiserum against PARP-1 was generated in-house using a purified recombinant antigen comprising the amino-terminal half of PARP-1 (3) (now available from Active Motif; catalog no. 39559). The other antibodies used were as follows: FLAG (Sigma-Aldrich, F3165), histone H2B (Abcam, ab1790), histone H3 (Abcam, ab1791), histone H4 (Abcam, ab10158), pan-acetyl-histone H2B (Millipore, 07-373), acetyl-histone H2B K12 (Abcam, ab195494), acetyl-histone H2B K20 (Cell Signaling, 34156), acetyl-histone H2B K120 (Active motif, 39120), phospho-histone H2A.X Ser139 (Millipore, 05-636), acetyl-histone H3 K27 (Abcam, ab4729), p300 (Active Motif, 61401), phospho-p53 Ser15 (Cell Signaling, 9284), p53 (Cell Signaling, 2524), β-actin (Cell Signaling, 3700), goat anti-rabbit HRP-conjugated IgG (ThermoFisher, 31460), and goat anti-mouse HRP-conjugated IgG (ThermoFisher, 31430).

Generation of lentiviral expression vectors for wild-type and site mutant histones

Double-stranded cDNAs encoding carboxyl-terminal FLAG epitope-tagged human wild-type and site-mutant histones H2B, H2A, H3, and H4 were synthesized as gene blocks (Integrated DNA Technologies), and then cloned individually into pCDH-EF1α-MCS-IRES-Puro lentiviral expression vector using Gibson assembly (NEB, E2621). Twenty-five individual glutamate (Glu, E) and aspartate (Asp, D) oncohistone sites (4) as follows were mutated into alanine (Ala, A). H2B-D51 and H4-D68 were also mutated into asparagine (Asn, N).

- H2B: E2, E35, D51, D68, E71, E76, E93, E113
- H2A: E56, E61, E92, E121

- H3: E50, E73, D81, E97, E105, D106, D123, E133
- H4: E52, E53, E63, D68, D85

Generation of stable ectopic protein expression cell lines

Lentiviruses were generated by transfecting the pCDH vectors described above into 293T cells, together with the expression vectors for the VSV-G envelope protein (pCMV-VSV-G, Addgene plasmid no. 8454), the expression vector for GAG-Pol-Rev (psPAX2, Addgene plasmid no. 12260), and a vector to aid with translation initiation (pAdVAntage, Promega) using Lipofectamine 3000 transfection reagent (Thermo Fisher Scientific, L3000015) according to the manufacturer's instructions. The viruses were collected in the culture medium, concentrated using a Lenti-X concentrator (Clontech, 631231), and used to infect four cancer cell lines: MCF-7, MDA-MB-231, OVCAR-3 and MDA-MB-468, and two normal cell lines: MCF-10A and FT-194. The infected cells were selected with 2 μg/mL puromycin (Sigma-Aldrich, P9620), expanded, and frozen in aliquots for future use. Ectopic expression of the cognate proteins was confirmed by Western blotting.

Cell proliferation assays

Cell proliferation assays were performed using a crystal violet staining assay. MCF-7, MDA-MB-231, OVCAR-3, MCF-10A and FT-194 cells ectopically expressing FLAG-tagged wild-type or mutant histones by lentivirus-mediated delivery were plated at a density of 4 x 10^4 cells per well in six well plates. The cells were collected at 1, 3, 5, and 7 days. After collection, the cells were washed with PBS, fixed for 10 minutes with 10% formaldehyde at room temperature, and stored in PBS at 4°C until all time points were collected. The fixed cells were stained with a solution containing 0.1% crystal violet in 20% methanol. After washing to remove unincorporated stain, the crystal violet was extracted using 10% glacial acetic acid and the absorbance was read at 595 nm. All proliferation assays were performed a minimum of three times to ensure reproducibility.

Cell migration assays

Cell culture inserts (Corning, 353097) were placed in a 24-well cell culture plate, forming migration chambers. MDA-MB-231 cells ectopically expressing FLAG-tagged wild-type or mutant H2B by lentivirus-mediated delivery were seeded at a density of 5 x 10^4 cells/mL following the manufacturer's protocol. Briefly, 5 x 10^4 cells in 250 μL of serum-free RPMI-1640 medium were plated into the top chamber. The chambers were then incubated in 750 μL of RPMI-1640 media containing 10% FBS. After 24 hours of incubation at 37ºC, the cells in the top chamber were removed. The chambers were stained with crystal violet (0.5% crystal violet in 20% methanol) for 5 minutes with gentle shaking, and then washed with water and air-dried. Images of cells at the bottom of the membrane were collected using an upright microscope. All migration assays were performed three times to ensure reproducibility. Statistical differences were determined using Student's t-test.

Preparation of cell extracts and Western blotting

Preparation of whole cell, nuclear, and cytosolic extracts was performed as described previously (5).

Preparation of whole cell lysates. Cells were collected, washed with ice-cold PBS, and resuspended in MNase Whole Cell Lysis Buffer [50 mM Tris-HCl pH 7.9, 2 mM $CaCl_2$, 0.2%

Triton X-100, 100 U/mL micrococcal nuclease (Worthington, LS004797), 1x complete protease inhibitor cocktail (Roche, 11697498001), 250 nM ADP-HPD (Sigma-Aldrich, A0627, a PARG inhibitor), 10 μM PJ34 (Enzo Life Sciences, ALX-270-289, a PARP inhibitor)] and incubated for 15 minutes at room temperature with gentle mixing to lyse the cells and extract the proteins. After brief sonication, the lysates were clarified by centrifugation in a microcentrifuge for 5 minutes at 4°C at full speed.

Preparation of cell fractions. Cells were collected, washed with ice-cold PBS, and resuspended in Isotonic Buffer (10 mM Tris-HCl pH 7.5, 2 mM $MgCl_2$, 3 mM $CaCl_2$, 0.3 M sucrose, with freshly added 1 mM DTT, 250 nM ADP-HPD, and 10 μM PJ34), incubated on ice for 15 minutes, and lysed by the addition of 0.6% IGEPAL CA-630 with gentle vortexing. After centrifugation (800 x *g*, 5 min, 4°C), the supernatant was collected as the cytoplasmic fraction. The pelleted nuclei were resuspended in Nuclear Extraction Buffer (20 mM HEPES pH 7.9, 1.5 mM $MgCl_2$, 0.42 M NaCl, 0.2 mM EDTA, 25% v/v glycerol, with freshly added 1 mM DTT, 1x phosphatase inhibitor cocktail, 250 nM ADP-HPD, and 10 μM PJ34) and incubated on ice for 30 minutes. The chromatin and soluble nuclear fractions were separated by centrifugation (12,000 x *g*, 30 min, 4°C). The chromatin fraction was then resuspended in Chromatin Extraction Buffer (10 mM Tris-HCl pH 7.5, 10 mM KCl, 1 mM $CaCl_2$, 1x protease inhibitor cocktail, 250 nM ADP-HPD, and 10 μM PJ34) and then digested with micrococcal nuclease (40 U/ml) at 37°C for 15 min. The reaction was stopped by the addition of 5 mM EGTA, and the chromatin fraction was collected by centrifugation (12,000 x *g*, 30 min, 4°C).

Determination of protein concentrations and Western blotting. Protein concentrations were determined using a BCA protein assay (Pierce, 23225). The cell extracts were aliquoted, flash-frozen in liquid N_2, and stored at −80°C. Aliquots of the cell extracts were run on polyacrylamide-SDS gels and transferred to nitrocellulose membranes. After blocking with 5% nonfat milk in TBST, the membranes were incubated with the primary antibodies described above in 3% nonfat milk prepared in TBST, followed by anti-rabbit HRP-conjugated IgG or anti-mouse HRP-conjugated IgG. Western blot signals were detected using an ECL detection reagent (Thermo Fisher Scientific, 34077, 34095).

Nucleosome immunoprecipitation

Nucleosome isolation was performed using micrococcal nuclease as described previously (5,6). MDA-MB-231 cells ectopically expressing FLAG-tagged wild-type or mutant histones by lentivirus-mediated delivery were seeded at ~5×10^6 cells per 15 cm diameter plate and cultured as described above. Nucleosome isolation was performed as described previously (6). Briefly, the cells were collected and the nuclei were isolated using Hypotonic Buffer (5 mM HEPES pH 7.5, 10 mM KCl, 5 mM $MgCl_2$, 0.5 mM EDTA, 0.4 mM PMSF, with freshly added 1 mM DTT, 1x protease inhibitor cocktail, 250 nM ADP-HPD, and 10 μM PJ34), followed by centrifugation (1350 x *g*, 5 min, 4°C). The nuclei were resuspended in Buffer A (15 mM HEPES pH 7.5, 30 mM KCl, 3 mM $CaCl_2$, 3 mM $MgCl_2$, 0.4 mM PMSF, with freshly added 1 mM DTT, 1x protease inhibitor cocktail, 250 nM ADP-HPD, and 10 μM PJ34) and incubated with 40 U/mL micrococcal nuclease (Worthington, LS004797) at 37°C for 15 minutes. The micrococcal nuclease reaction was stopped by adding 5 mM EDTA, 3 mM EGTA, and 200 mM KCl (final concentrations). After centrifugation at 10,000 x *g* for 15 minutes at 4°C, the supernatant containing the soluble chromatin (mainly mononucleosomes) was collected, and the concentration was determined using a BCA protein assay. One mg of chromatin extract protein was incubated with anti-FLAG M2 agarose resin (Sigma-Aldrich, A2220) for 4 hours at 4°C and then washed 3 times with Wash Buffer (10

mM HEPES pH 7.5, 300 mM KCl, 0.5 mM EDTA, 0.1% Tween 20). The mononucleosomes were recovered from the beads by heating to 100°C for 5 minutes in 2 x SDS-PAGE loading buffer. The immunoprecipitated material was subjected to Western blotting as described above.

Identification of histone PTMs by mass spectrometry

Processing of native nucleosomes isolated from MCF-7 cells for identification of histone ADPRylation sites. MCF-7 cells were seeded at ~5×10^6 cells per 15 cm diameter plate and cultured as described above. Nucleosome isolation was performed using micrococcal nuclease as described previously (6). Isolated mononucleosomes were incubated in 200 mM HEPES pH 8.8 in the presence of 0.75 M hydroxylamine (Sigma, 438227) at 4°C for 16 hours. The mononucleosomes were concentrated using centrifugal filter units (Millipore, UFC501024), and electrophoresed on a precast SDS-PAGE gel. The regions containing histone proteins were excised from the gel. The gel pieces were reduced and alkylated with DTT (20 mM) and iodoacetamide (27.5 mM), respectively (Sigma–Aldrich). A 0.01 µg/µL solution of trypsin in 50 mM triethylammonium bicarbonate (TEAB) was added to completely cover the gel slices and with incubation at room temperature overnight. The samples were then subjected to solid-phase extraction cleanup with an Oasis HLB µelution plate (Waters), the resulting peptides were reconstituted in 10 µL of 2% (v/v) acetonitrile (ACN) and 0.1% trifluoroacetic acid in water.

Processing of nucleosomes isolated from MDA-MB-231 cells expressing FLAG-tagged wild-type or mutant histone H2B for identification of histone PTMs. MDA-MB-231 cells expressing FLAG-tagged wild-type or mutant histone H2B were seeded at ~5×10^6 cells per 15 cm diameter plate and cultured as described above. Nucleosome immunoprecipitation was performed as described above. The immunoprecipitated material was electrophoresed on a precast SDS-PAGE gel and the regions containing histone proteins were excised from the gel. The gel pieces were reduced and alkylated with DTT (20 mM) and iodoacetamide (27.5 mM), respectively (Sigma-Aldrich). A 0.01 µg/µL solution of trypsin in 50 mM triethylammonium bicarbonate (TEAB) was added to completely cover the gel slices and with incubation at room temperature overnight. The samples were then subjected solid-phase extraction cleanup with an Oasis HLB µelution plate (Waters), the resulting peptides were reconstituted in 10 µL of 2% (v/v) acetonitrile (ACN) and 0.1% trifluoroacetic acid in water.

Identification of histone PTMs by mass spectrometry. Five µL of the peptide solution were injected onto an Orbitrap Fusion Lumos mass spectrometer (Thermo Electron) coupled to an Ultimate 3000 RSLC-Nano liquid chromatography system (Dionex). The samples were injected onto a 75 µm i.d., 75-cm long EasySpray column (Thermo), and eluted with a gradient from 1-28% Buffer B over 90 minutes. Buffer A contained 2% (v/v) ACN and 0.1% formic acid in water, and Buffer B contained 80% (v/v) ACN, 10% (v/v) trifluoroethanol, and 0.1% formic acid in water.

The mass spectrometer was operated in positive ion mode with an ion transfer tube temperature of 275°C. MS scans were acquired at 120,000 resolution in the Orbitrap and up to 10 MS/MS spectra were obtained in the ion trap for each full spectrum acquired using higher-energy collisional dissociation (HCD) for ions with charges 2-7. Dynamic exclusion was set for 25 s after an ion was selected for fragmentation. Raw MS data files were analyzed using Proteome Discoverer v2.2 (Thermo), with peptide identification performed using Sequest HT searching against the human protein database from UniProt. Fragment and precursor tolerances of 10 ppm and 0.6 Da were specified, and three missed cleavages were allowed. Carbamidomethylation of Cys was set as a fixed modification, with oxidation of Met set as a variable modification. For detection of ADPRylation sites, hydroxamic acid addition (+15.0109 Da) to Asp and Glu were set

as variable modifications. For detection of PTM sites, acetylation of Lys, mono, di, and trimethylation of Lys and Arg, phosphorylation of Ser, Thr, and Tyr, and ubiquitylation of Lys were set as variable modifications. The false-discovery rate (FDR) cutoff was 1% for all proteins and peptides.

Expression and purification of recombinant proteins

Purification of PARP-1 expressed in Sf9 insect cells. PARP-1 was purified from Sf9 insect cells as described (5). The cells were cultured in SF-II 900 medium (Invitrogen), and transfected with 1 μg of bacmid driving expression of FLAG-tagged wild-type human PARP-1 using Cellfectin transfection reagent (Invitrogen) as described by the manufacturer. After three days, the medium was supplemented with 10% FBS, penicillin, and streptomycin, and collected as a baculovirus stock. After multiple rounds of amplification of the stock, the resulting high titer baculovirus was used to infect fresh Sf9 cells to induce expression of PARP-1 protein for two days. PARP-1-expressing Sf9 cells were collected by centrifugation, flash frozen in liquid N_2, and stored at -80°C.

For purification of PARP-1 (5), the Sf9 cell pellets were thawed on wet ice. The cells were resuspended in FLAG Lysis Buffer (20 mM HEPES pH 7.9, 0.5 M NaCl, 4 mM $MgCl_2$, 0.4 mM EDTA, 20% glycerol, 250 mM nicotinamide, 2 mM β-mercaptoethanol, 2x protease inhibitor cocktail) and lysed by Dounce homogenization (Wheaton). The lysate was clarified by centrifugation (15,000 rpm, 30 min, 4°C), mixed with an equal volume of FLAG Dilution Buffer (20 mM HEPES pH 7.9, 10% glycerol, 0.02% NP-40), sonicated, and then clarified by centrifugation (15,000 rpm, 30 min, 4°C) again. The clarified lysate was mixed with anti-FLAG M2 agarose resin (Sigma-Aldrich, A2220), washed twice with FLAG Wash Buffer #1 (20 mM HEPES pH 7.9, 150 mM NaCl, 2 mM $MgCl_2$, 0.2 mM EDTA, 15 % glycerol, 0.01% NP-40, 100 mM nicotinamide, 0.2 mM β-mercaptoethanol, 1 mM PMSF, 1 μM aprotinin, 100 μM leupeptin), twice with FLAG Wash Buffer #2 (20 mM HEPES pH 7.9, 1 M NaCl, 2 mM $MgCl_2$, 0.2 mM EDTA, 15% glycerol, 0.01% NP-40, 100 mM nicotinamide, 0.2 mM β-mercaptoethanol, 1 mM PMSF, 1 μM aprotinin, 100 μM leupeptin), and twice with FLAG Wash Buffer #3 (20 mM HEPES pH 7.9, 150 mM NaCl, 2 mM $MgCl_2$, 0.2 mM EDTA, 15% glycerol, 0.01% NP-40, 0.2 mM β-mercaptoethanol, 1 mM PMSF). The FLAG-tagged PARP-1 protein was eluted from the anti-FLAG M2 agarose resin with FLAG Wash Buffer #3 containing 0.5 mg/mL 3x FLAG peptide (Sigma-Aldrich, F4799). The eluted proteins were aliquoted, flash frozen in liquid N2, and stored at -80°C until used. To assess the purity and quality of the purified proteins, the purified protein was subjected to SDS-PAGE and stained with Coomassie Brilliant Blue.

Purification of p300 expressed in Sf9 insect cells. p300 was purified from Sf9 insect cells as described (7). Sf9 cells were infected with baculovirus driving the expression of FLAG-tagged p300 for 48 hours at the Protein and Monoclonal Antibody Production Shared Resource at Baylor College of Medicine. The Sf9 cells were treated for 3 hours prior to harvesting with the following p300 inhibitors: 10 μM SGC-CBP30 (Sigma-Aldrich, SML1133), 25 μM C646 (Sigma-Aldrich, SML0002), and 10 μM of A-485 (Tocris, 6387). After 48 hours of incubation, the cells were collected by centrifugation. The cells were resuspended in Flag-p300 Lysis Buffer (20 mM Tris-HCl pH 7.9, 0.5 M NaCl, 4 mM $MgCl_2$, 5 μM $ZnCl_2$, 20% glycerol, 2 mM β-mercaptoethanol, 2x protease inhibitor cocktail) and lysed by Dounce homogenization and sonication. The lysate was clarified by centrifugation using an SS-34 rotor in a Sorvall centrifuge at 15,000 RPM for 30 minutes at 4°C and mixed with an equal volume of Flag-p300 Dilution Buffer (20 mM Tris-HCl pH 7.9, 10% glycerol, 0.02% NP-40, 5 μM $ZnCl_2$). The diluted lysate was incubated for 3 hours

with anti-Flag M2 agarose resin and washed five times with Flag-p300 Wash Buffer (20 mM Tris-HCl pH 7.9, 200 mM NaCl, 2 mM $MgCl_2$, 5 μM $ZnCl_2$, 15 % glycerol, 0.1% NP-40, 0.2 mM β-mercaptoethanol, 1 mM PMSF, 1 μM aprotinin, 100 μM leupeptin). The Flag-tagged p300 protein was eluted from the anti-Flag M2 agarose resin with Flag-p300 Elution Buffer (20 mM Tris-HCl pH 7.9, 100 mM NaCl, 2 mM $MgCl_2$, 5 μM $ZnCl_2$, 15 % glycerol, 0.01% NP-40, 0.2 mM β-mercaptoethanol, 1 mM PMSF) containing 0.2 mg/mL 3x Flag peptide, flash frozen in liquid N_2, and stored at -80°C. To assess the purity and quality of the purified proteins, the purified protein was subjected to SDS−PAGE and stained with Coomassie Brilliant Blue.

Purification of histone H2B expressed in E. coli. The human histone H2B cDNA was cloned into pRUTH5 to yield an N-terminal His6-TEV tagged version of the cDNA. To generate recombinant H2B(D51A) and H2B(D51N), mutations were introduced into the pRUTH5-H2B construct using standard site-directed mutagenesis with the primers listed below. H2B was then expressed in BL21(DE3) *E. coli*. The transformed bacteria were grown in LB containing ampicillin at 37°C and the expression of recombinant protein was induced by the addition of 1 mM IPTG for 4 h at 37°C. The cells were collected by centrifugation and lysed by tip sonication in Wash/Lysis (WL) Buffer (50 mM Tris-HCl pH 8.0, 500 mM NaCl, 10 mM imidazole, 5-10% (v/v) glycerol, 10 mM β-mercaptoethanol, 1mM PMSF, 1-5 U/mL Benzonase) until no longer viscous.

The lysates were centrifugated at 15,000 rpm using an SS34 rotor (Sorvall) at 4°C for 20 minutes to collect inclusion bodies, which were solubilized once in WL buffer with 1% triton X-100 and once in WL without triton X-100 by vortexing. After centrifugation, the pellet was resuspended in DMSO to partially dissolve it and then in Buffer D500 (50 mM Tris-HCl pH 8, 6.3 M guanidine-HCl, 500 mM NaCl, 10 mM β-mercaptoethanol, adjusted with NaOH/1 M Tris base to pH 8.0), vortexed, and rotated for 1 hour. After centrifugation, the supernatant was incubated with Ni-NTA resin equilibrated in Buffer D500 at 4°C for 2 hours with gentle mixing. The resin was packed into columns, drained, and washed once with Buffer D500 and twice with Buffer D1000 (Buffer D500 with 1000 mM NaCl final concentration). The recombinant proteins were eluted twice in Elution Buffer (D1000 + 300 mM imidazole) and dialyzed in Dialysis Buffer (1% acetoacetate, 5 mM β-mercaptoethanol) at 4°C overnight. The dialyzed proteins were quantified using a Bradford protein assay (Bio-Rad), aliquoted, flash-frozen in liquid N_2, and stored at -80°C. To assess the purity and quality of the purified proteins, they were subjected to SDS-PAGE and stained with Coomassie Brilliant Blue.

To generate recombinant H2B(D51A) and H2B(D51N), mutations were introduced into the pRUTH5-H2B construct using standard site-directed mutagenesis using the following primers:
- H2B(D51A) For: 5'-GTGCTGAAGCAGGTCCACCCCGCCACCGGCATCTCCTCTAAGGC-3'
- H2B(D51A) Rev: 5'- GCCTTAGAGGAGATGCCGGTGGCGGGGTGGACCTGCTTCAGCAC-3'
- H2B(D51N) For: 5'-GTGCTGAAGCAGGTCCACCCCAACACCGGCATCTCCTCTAAGGC-3'
- H2B(D51N) Rev: 5'-GCCTTAGAGGAGATGCCGGTGTTGGGGTGGACCTGCTTCAGCAC-3'

Purification of NMNAT-1 expressed in E. coli. NMNAT-1 was purified from *E.coli* as described (5). 6x His-tagged human NMNAT-1 (UniProt entry Q9EPA7) was expressed in *E. coli* strain BL21(DE3) using a pET19b-based bacterial expression vector (5). The transformed bacteria were grown in LB containing ampicillin at 37°C until the OD595 reached 0.4−0.6. Recombinant protein expression was induced by the addition of 1 mM IPTG for 2 h at 37°C. The cells were collected by centrifugation, and the cell pellets were flash-frozen in liquid N_2 and stored at −80°C. The frozen cell pellets were thawed on wet ice and lysed by sonication in Ni-NTA Lysis Buffer (10 mM Tris-HCl pH 7.5, 0.5 M NaCl, 0.1 mM EDTA, 0.1% NP-40, 10% glycerol, 10 mM imidazole, 1 mM PMSF, and 1 mM β-mercaptoethanol). The lysates were clarified by

centrifugation at 15,000 rpm using an SS34 rotor (Sorvall) at 4°C for 45 minutes. The supernatant was incubated with 1 mL of Ni-NTA resin equilibrated in Ni-NTA Equilibration Buffer (10 mM Tris-HCl pH 7.5, 0.5 M NaCl, 0.1% NP-40, 10% glycerol, 10 mM imidazole, and 1 mM β-mercaptoethanol) at 4°C for 2 hours with gentle mixing. The resin was collected by centrifugation at 4°C for 10 minutes at 1,000 x *g*, and the supernatant was removed. The resin was washed three times with Ni-NTA Wash Buffer (10 mM Tris-HCl pH 7.5, 1 M NaCl, 0.2% NP-40, 10% glycerol, 10 mM imidazole, and 1 mM PMSF). The recombinant proteins were then eluted using Ni-NTA Elution Buffer (10 mM Tris-HCl pH 7.5, 0.2 M NaCl, 0.1% NP-40, 10% glycerol, 500 mM imidazole, 1 mM PMSF, and 1 mM β-mercaptoethanol). The eluates were collected by centrifugation at 4°C for 10 minutes at 1,000 x *g*, and dialyzed in Ni-NTA Dialysis Buffer (10 mM Tris-HCl pH 7.5, 0.2 M NaCl, 10% glycerol, 10 mM imidazole, 1 mM PMSF, and 1 mM β-mercaptoethanol). The dialyzed proteins were quantified using a Bradford protein assay (Bio-Rad), aliquoted, flash-frozen in liquid N_2, and stored at -80°C.

In vitro PARylation assays

In vitro PARylation assays were performed essentially as described previously (5,8,9). One μg of purified human H2B protein or 500 nM of assembled human mononucleosomes (EpiCypher, 16-0009) were mixed with 0.1 μM purified human PARP-1, 1 μM purified human NMNAT-1, 100 μM NAD^+, and 100 μM ATP in Reaction Buffer (50 mM Tris-HCl pH 7.4, 10 mM $MgCl_2$, 5% glycerol, and 1 mM DTT). The PARylation reactions were initiated by adding 25-mer DNA, incubated at room temperature for 20 minutes, and then stopped by the addition of one third of a reaction volume of 4x SDS-PAGE Loading Buffer followed by heating to 100°C for 5 minutes. To perform subsequent HAT assays, the PARylation reactions were stopped by the addition of 10 μM PJ34, followed by the addition of p300 and acetyl-CoA as described below. The reaction products were then subjected to Western blotting as described above.

In vitro HAT assays

One μg of purified human H2B protein or 500 nM of assembled human mononucleosomes (EpiCypher, 16-0009) were incubated with purified p300 protein (50 ng) in Reaction Buffer (50 mM Tris-HCl pH 7.4, 10 mM $MgCl_2$, 5% glycerol, and 1 mM DTT) in the presence of 25 μM acetyl-CoA. The HAT reactions were incubated at 30°C for 30 min and stopped by the addition of one third of a reaction volume of 4x SDS-PAGE Loading Buffer (200 mM Tris•HCl, pH 6.8, 8% SDS, 40% glycerol, 4% β-mercaptoethanol, 50 mM EDTA, 0.08% bromophenol blue), followed by heating to 100°C for 5 minutes. The reaction products were then subjected to Western blotting as described above.

RNA-sequencing and data analysis

The following methods were used to generate, evaluate for QC, sequence, and analyze the RNA-seq data.

Generation and sequencing of RNA-seq libraries. MDA-MB-231 cells expressing FLAG-tagged wild-type or mutant histones were seeded in 6-well plates. The cells were collected and total RNA was isolated using the RNeasy kit (Qiagen, 74136) according to the manufacturer's instructions. The total RNA was then enriched for polyA+ RNA using Dynabeads Oligo(dT)25 (Life Technologies, 61002). The polyA+ RNA was then used to generate strand-specific RNA-seq libraries as described previously (10). The RNA-seq libraries were subjected to QC analyses (i.e., number of PCR cycles required to amplify each library, the final library yield, and the size

distribution of final library DNA fragments) and sequenced using an Illumina NextSeq 500 to an average depth of ~40 million reads total per condition. Two independent biological replicates with two sets of sequencing replicates were used.

Analysis of RNA-seq data. The quality of RNA-seq datasets was assessed using the FastQC tool (http://www.bioinformatics.babraham.ac.uk/projects/fastqc) and the reads were then mapped to the human reference genome (hg38) using the spliced read aligner TopHat (v2.0.13) (11). Uniquely mapped reads were converted into bigwig files using the RSeQC tool (v2.6.4) (12) for visualization. Transcriptome assembly was performed using cufflinks (v2.2.1) with default parameters (13). The transcripts were further merged into distinct, non-overlapping sets using cuffmerge, followed by cuffdiff to call the differentially regulated transcripts. The genes with FPKM > 1 in either WT or mutant (D51A or D51N) H2B conditions were collected for further analysis. An FDR cutoff of 0.05 and a fold change cutoff of 1.5 was used to determine significantly regulated genes in mutants compared to the WT H2B condition.

Gene ontology (GO) analyses. Gene ontology analyses were performed on the differentially-expressed gene sets using DAVID (Database for Annotation, Visualization, and Integrated Discovery) (14). DAVID returns clusters of related ontological terms that are ranked according to an enrichment score. The top GO biological process terms from these clusters based on the enrichment score were listed. The gene body scaled metaplots for the commonly upregulated and downregulated genes were plotted using deepTools (v2.3.5) (15).

ATAC- sequencing and data analysis

Generation and sequencing of ATAC-seq libraries. ATAC-seq was performed using the Omni-ATAC protocol as previously described (16). MDA-MB-231 cells expressing FLAG-tagged wild-type or mutant histones were seeded in 6-well plates. For individual samples, 5 x 10^4 cells were collected, washed, and lysed in 50 µL of cold ATAC Resuspension Buffer (10 mM Tris-HCl pH 7.4, 10 mM NaCl, 3 mM $MgCl_2$, 0.1% NP-40, 0.1% Tween-20, and 0.01% digitonin) on ice. Nuclei were then collected and resuspended in 50 µL of Transposition Mixture (10 mM Tris-HCl pH 7.6, 3 mM $MgCl_2$, 10% dimethylformamide, 100 nM transposase, 0.1% Tween-20, and 0.01% digitonin), and incubated at 37°C for 30 minutes in a thermomixer at 1,000 RPM. DNA was collected using a Qiaquick PCR purification kit (Qiagen, 28104) according to the manufacturer's instructions. Eluted DNA was amplified using a KAPA non-hot-start PCR kit and purified using AMPure XP beads. The ATAC-seq libraries were subjected to QC analyses (i.e., the final library yield and the size distribution of the final library DNA fragments) and sequenced using an Illumina NextSeq 500 to an average depth of 57 million unique aligned reads per each biological replicate. Two independent biological replicates with three sets of sequencing replicates were used.

Analysis of ATAC-seq data. The quality of the ATAC-seq datasets was assessed using the FastQC tool (http://www.bioinformatics.babraham.ac.uk/projects/fastqc). The ATAC-seq reads were then aligned to the human genome (hg38) using BWAKit (v0.7.15) (17). For unique alignments, duplicate reads with quality score over 10 were filtered out using picard tools (v2.10.3) (http://broadinstitute.github.io/picard/). The resulting uniquely mapped reads were normalized to the same read depth across all samples and converted into bigWig files using the writeWiggle function from the groHMM package in R (18) for visualization in the UCSC Genome Browser. Peak calling was performed using MACS2 with default parameters (19,20). The read counts under the ATAC-seq peak calls were calculated using featureCounts for each replicate and the peaks with read counts greater than 10 were selected further as an input to determine differentially

enriched peaks using DESseq2 software (21) using an FDR cutoff of 0.05 and a fold change (FC) cutoff of ≥ 1.5.

Motif searching on the differentially enriched ATAC-seq peaks was performed using findMotifsGenome.pl program using HOMER (Heinz et al., 2010) motif discovery algorithm. To analyze footprinting signatures in ATAC-seq data the TOBIAS package was used (v0.12.10; available at https://github.com/loosolab/TOBIAS/) (22). Merged BAM files from each condition were processed using ATACorrect, footprint scores calculated using FootprintScores. The footprinting analysis on differential accessible regions from the ATAC-seq peaks was performed using BINDetect.

Crosslinked chromatin immunoprecipitation (ChIP) and ChIP-qPCR

MDA-MB-231 cells expressing inducible FLAG-tagged wild-type or mutant histone H2B were seeded at ~$5x10^6$ cells per 15 cm diameter plate. The cells were treated with 10 μM Niraparib, or vehicle for 2 hours.

Crosslinked chromatin immunoprecipitation. Formaldehyde crosslinked ChIP was performed as described previously (23,24), with a few modifications. Briefly, the cells were crosslinked with 1% formaldehyde in PBS for 10 min at 37°C and quenched in 125 mM glycine in PBS for 5 min at 4°C. The cells were then collected and lysed in Farnham Lysis Buffer (5 mM PIPES pH 8.0, 85 mM KCl, 0.5% NP-40, with freshly added 1 mM DTT, 1x protease inhibitor cocktail, 1x phosphatase inhibitor cocktail, 250 nM ADP-HPD, and 10 mM PJ34). The crude nuclear pellet was collected by centrifugation, resuspended in Chromatin Lysis Buffer (50 mM Tris-HCl pH 7.9, 1% SDS, 10 mM EDTA, with freshly added 1 mM DTT, 1x protease inhibitor cocktail, 1x phosphatase inhibitor cocktail, 250 nM ADP-HPD, and 10 mM PJ34), and incubated on ice for 10 min. The chromatin was sheared at 4°C by sonication using a Bioruptor UC200 to generate chromatin fragments of ~300 bp in length. The soluble chromatin was diluted 1:10 with Dilution Buffer (20 mM Tris-HCl pH 7.9, 0.5% Triton X-100, 2 mM EDTA, 150 mM NaCl, with freshly added 1 mM DTT, 1x protease inhibitor cocktail, 1x phosphatase inhibitor cocktail, 250 nM ADP-HPD and 10 mM PJ34) and pre-cleared with protein A-agarose beads.

The pre-cleared lysates were incubated with antibodies against the factor of interest (PARP-1, p300, or H2BK12ac) at 4°C overnight. Twenty mL of protein A-agarose beads were then added to the sample with continue incubation for an extra 2 hours at 4°C with constant mixing. The immunoprecipitated material was then washed once with Low Salt Wash Buffer (20 mM Tris-HCl pH 7.9, 2 mM EDTA, 125 mM NaCl, 0.05% SDS, 1% Triton X-100, with freshly added 1x protease inhibitor cocktail, and 1x phosphatase inhibitor cocktail), once with High Salt Wash Buffer (20 mM Tris-HCl pH 7.9, 2 mM EDTA, 500 mM NaCl, 0.05% SDS, 1% Triton X-100, with freshly added 1x protease inhibitor cocktail, and 1x phosphatase inhibitor cocktail), once with LiCl Wash Buffer (10 mM Tris-HCl pH 7.9, 1 mM EDTA, 250 mM LiCl, 1% NP-40, 1% sodium deoxycholate, with freshly added 1x protease inhibitor cocktail, and 1x phosphatase inhibitor cocktail), and once with 1x Tris-EDTA (TE). The immunoprecipitated material was eluted in Elution Buffer (100 mM NaHCO3, 1% SDS), de-crosslinked overnight at 65°C, and then digested with proteinase K and RNase H to remove protein and RNA, respectively. The immunoprecipitated genomic DNA was then extracted with phenol:chloroform:isoamyl alcohol and precipitated with ethanol.

ChIP-qPCR. The ChIPed genomic DNA was subjected to qPCR using a LightCycler® 480 Instrument II system and Power SYBR Green PCR master mix. All experiments were performed at least three separate biological replicates to ensure reproducibility. Statistical

differences between two groups were determined using the Student's t test and a statistical significance was defined as $p < 0.05$. The ChIP-qPCR assays for *TFF1* and *GAPDH* shown in Fig. S10 were performed using native ChIP of H2BK12ac (see below), but processed for qPCR as described here. The qPCR primer sequences used in this study are listed here:

- *PMEPA1* Forward: 5'-GGACCCCATGGAAGTCAGTG-3'
- *PMEPA1* Reverse: 5'-TTGGCTCAGTCAGGCACTTT-3'
- *SOST* Forward: 5'-CAAATGGCCCAAGGCGTTTC-3'
- *SOST* Reverse: 5'-GGAGTTGGGACCAATGGGATT-3'
- *SEMA3B* Forward: 5'-CCCACTGGCCCCTGTTATTT-3'
- *SEMA3B* Reverse: 5'-AAGTGGAAGTGGGGCTATGC-3'
- *LEFTY1* Forward: 5'-ACTCTGGCATCATCAGGGGTC-3'
- *LEFTY1* Reverse: 5'-CTGAAACGGGTCCCTATTCCTG-3'
- *ASB2* Forward: 5'-CAAAATCGATTCCGCCCCAC-3'
- *ASB2* Reverse: 5'-TCACATGTGTCTCACGGCAC-3'
- *TFF1* Forward: 5'-GTTGGGAGCTAGGATGGTCA-3'
- *TFF1* Reverse: 5'-AGTGAGTGGCGGATTTGAAC-3'
- *GAPDH* Forward: 5'-TGAAAGAAAGAAAGGGGAGGGG-3'
- *GAPDH* Reverse: 5'-AGCAGGACACTAGGGAGTCAA-3'

Native ChIP and ChIP-sequencing

MDA-MB-231 cells expressing inducible FLAG-tagged wild-type or mutant histone H2B were seeded at ~$5x10^6$ cells per 15 cm diameter plate. The cells were treated with 5 μM A485 or vehicle for 2 hours. Native ChIP was performed as previously described using with 5×10^6 cells (25). A spike-in strategy was used to normalize all ChIP-seq data to reduce the effects of technical variation and sample processing bias. Spike-In chromatin (Active Motif, 53083) and Spike-in antibody (Active Motif, 61686) were used according to manufacturer instructions.

Native chromatin immunoprecipitation. The cells were trypsinized to release them from the culture dishes, washed, and lysed using Hypotonic Lysis Buffer [50 mM Tris-HCl pH 7.4, 1 mM $CaCl_2$, 0.2% Triton X-100, 250 nM ADP-HPD (Sigma-Aldrich, A0627, a PARG inhibitor), 10 μM PJ34 (Enzo Life Sciences, ALX-270-289, a PARP inhibitor), and protease inhibitor cocktail (Roche)] with micrococcal nuclease for 5 min at 37°C to recover mono- to tri-nucleosomes. Nuclei were lysed by brief sonication and dialyzed into RIPA Buffer (10 mM Tris pH 7.6, 1 mM EDTA, 0.1% SDS, 0.1% sodium deoxycholate, 1% Triton X-100) for 2 hours at 4°C. Soluble material (30 μg) was incubated with 2.5 μg of H2BK12ac antibody bound to 25 μL protein A Dynabeads (Invitrogen) and incubated overnight at 4°C, with 5% reserved as input. Magnetic beads were washed as follows: 3x RIPA buffer, 2x RIPA buffer + 300 mM NaCl, 2x LiCl Buffer (250 mM LiCl, 0.5% NP-40, 0.5% sodium deoxycholate), 1x TE + 50 mM NaCl. Chromatin was eluted and treated with Proteinase K. The ChIPed DNA was purified and eluted in water.

ChIP-seq library preparation. ChIP-seq libraries were prepared from 5 ng of ChIPed DNA following the Illumina TruSeq protocol. The quality of the libraries was assessed using a D1000 ScreenTape on a 2200 TapeStation (Agilent) and quantified using a Qubit dsDNA HS Assay Kit (Thermo Fisher). Libraries with unique adaptor barcodes were multiplexed and sequenced on an Illumina NextSeq 500 (paired-end, 33 base pair reads). The ChIP-seq libraries were sequenced to an average depth of ~35 million unique aligned reads per condition. Two independent biological replicates were used.

Analysis of ChIP-seq data. The quality of the ChIP-seq datasets was assessed using the

FastQC tool (http://www.bioinformatics.babraham.ac.uk/projects/fastqc). ChIP-seq raw reads were aligned separately to the human reference genome (hg38) and the spike-in *Drosophila* reference genome (dm3) using Bowtie2 (v2.3.2) (26). Only one alignment is reported for each read and duplicate reads were filtered using the Picard MarkDuplicates tool. Uniquely mapped *Drosophila* reads were counted in the sample containing the least number of *Drosophila* mapped reads and used to generate a normalization factor for random downsampling. Reads were converted into bigwig files using BEDTools (v2.29.0) genomecov function (27) for visualization in the UCSC Genome Browser. ChIP-seq peak calling was performed using the findPeaks function of HOMER (28) with an FDR cutoff of 0.001.

Integration, analysis, and visualization of ChIP-seq, ATAC-seq, and RNA-seq data

The up- or downregulated ATAC-seq peaks nearest to the transcription start sites (TSSs) of up- or downregulated regulated genes (from RNA-seq) were obtained using BEDTools closest function (27). The distance between the TSS and the nearest regulated ATAC-seq peak was represented as a histogram using the hist function in R. The metaplots of ATAC-seq and ChIP-seq data at the TSSs and nearest regulated ATAC-seq peaks were generated using the metagene function in the groHMM software package (18). Box plot representations were used to quantitatively represent the read distribution in a fixed 4 kb window (± 2000 bp) surrounding the TSS and the nearest regulated ATAC-seq peak using the box plot function in R. Wilcoxon rank sum tests were performed to determine the statistical significance of all comparisons.

To integrate ATAC-seq peaks with histone modifications, published histone PTM ChIP-seq data from MDA-MB-231 cells was obtained from the LONESTAR Consortium data sets (1). The coordinates of ATAC-seq peaks with higher or lower accessibility in cells expressing the H2B-D51N mutant compared to cells expressing H2B WT were lifted over to hg19. ChIP-seq reads in a ± 2 kb window around each ATAC-seq peak were calculated and normalized to sequencing depth to plot as boxplots using boxplot function in R. Wilcoxon rank sum tests were performed to determine the statistical significance between the two groups of ATAC-seq peaks for each histone modification. Average ChIP-seq profiles of the top three histone marks as observed in the boxplots were expressed as metaplots using the metaplot function in the groHMM package (18).

Immunofluorescent staining and confocal microscopy

MDA-MB-231 and MDA-MB-468 cells were seeded on eight-chambered cover slips (Thermo Fisher, 12-565-2) one day before treatment. The cells were treated with 2.5 μM Niraparib (MedChemExpress, HY-10619) or vehicle for 2 hours, or 5 mM H_2O_2 (Sigma-Aldrich, 216763) for 5 minutes followed by a 30-minute recovery in fresh media. The treated cells were washed three times with PBS, fixed with 4% paraformaldehyde for 15 minutes at room temperature, and washed three times with PBS. The cells were permeabilized for 5 minutes using Permeabilization Buffer (PBS containing 0.01% Triton X-100), washed three times with PBS, and blocked for 1 hour at room temperature in PBS containing 5% normal goat serum (Thermo Fisher Scientific, 50062Z) and 0.1% Tween-20. The cells were incubated overnight at 4°C with phospho-histone H2A.X Ser139 antibody (1:400, Millipore, 05-636) diluted in Blocking Solution. The cells were then washed three times with PBS, incubated with Alexa Fluor 488 goat anti-mouse IgG (1:500, ThermoFisher, A-11001) diluted in Blocking Solution for 1 hour at room temperature, and washed three more times with PBS. Finally, the coverslips were mounted with Anti-Fade mounting medium with DAPI (Vector Laboratories, H-1200). All images were acquired using an inverted

Zeiss LSM 780 confocal microscope (Live Cell Imaging Facility, UT Southwestern Medical Center).

Cell-derived xenograft experiments in mice

All animal use was performed with oversight from UT Southwestern's Institutional Animal Care and Use Committee. Mice were maintained on a standard rodent chow diet with 12-hour light and dark cycles. Female NOD *scid* gamma (NSG) mice at 6-8 weeks of age were used (The Jackson Laboratory, 005557). We used female mice because mammary cancers occur primarily in females. To establish breast cancer xenografts, 5×10^6 of MDA-MB-231 cells engineered for ectopic expression of FLAG-tagged histone H2B (WT or D51A mutant) were collected, washed, and resuspended in 100 μL of a 1:1 (v:v) solution of serum-free medium and Matrigel (Life Science, 354230), and then injected subcutaneously into the flanks of the mice. The tumors were allowed to form for 10-14 days.

Mice carrying ~100 mm^3 subcutaneous tumors were randomized to receive 25 mg/kg of Niraparib (MedChemExpress, HY-10619) in 4% DMSO, 5% PEG 300, 5%Tween-80 in PBS or an equal volume of vehicle intraperitoneally, 5 days a week (2 days off) for 4 weeks. The weight of the mice was monitored once a week and tumor growth measured using electronic calipers approximately every 7 days. Tumor volumes were calculated using a modified ellipsoid formula: Tumor volume = ½ (length × width × height). The experiment was terminated and the mice were euthanized as soon as the average tumor diameter measurement from any group exceeded 20 mm. Fresh tumor samples were flash frozen for later use.

For Western blotting, frozen tumor tissue was homogenized (PowerGen 125, Fisher Scientific) and lysed using MNase Whole Cell Lysis Buffer [50 mM Tris-HCl pH 7.9, 2 mM $CaCl_2$, 0.2% Triton X-100, 100 U/mL micrococcal nuclease (Worthington, LS004797), 1x complete protease inhibitor cocktail (Roche, 11697498001), 250 nM ADP-HPD (Sigma-Aldrich, A0627, a PARG inhibitor), 10 μM PJ34 (Enzo Life Sciences, ALX-270-289, a PARP inhibitor)] and incubated for 15 minutes at room temperature with gentle mixing to lyse the cells and extract the proteins. After brief sonication, the lysates were clarified by centrifugation in a microcentrifuge for 5 minutes at 4°C at full speed. Aliquots of the lysates were subjected to Western blotting as described above.

Quantification and statistical analysis

All sequencing-based genomic experiments were performed a minimum of two times with independent biological samples. Statistical analyses for the genomic experiments were performed using standard genomic statistical tests as described above. All qPCR-based gene specific experiments were performed a minimum of three times with independent biological samples. All Western blotting experiments with quantification were performed a minimum of three times with independent biological samples and analyzed by Image Lab 6.0. Statistical analyses were performed using GraphPad Prism 7. All tests and p-values are provided in the corresponding figures or figure legends. In all figures, the p values are shown as: *, $p < 0.05$; **, $p < 0.01$; ***, $p < 0.001$, ****, $p < 0.0001$.

5) Supplementary References

1. Xi Y, Shi J, Li W, Tanaka K, Allton KL, Richardson D*, et al.* Histone modification profiling in breast cancer cell lines highlights commonalities and differences among subtypes. BMC Genomics **2018**;19:150
2. Gibson BA, Conrad LB, Huang D, Kraus WL. Generation and Characterization of Recombinant Antibody-like ADP-Ribose Binding Proteins. Biochemistry **2017**;56:6305-16
3. Kim MY, Mauro S, Gevry N, Lis JT, Kraus WL. NAD+-dependent modulation of chromatin structure and transcription by nucleosome binding properties of PARP-1. Cell **2004**;119:803-14
4. Nacev BA, Feng L, Bagert JD, Lemiesz AE, Gao J, Soshnev AA*, et al.* The expanding landscape of 'oncohistone' mutations in human cancers. Nature **2019**;567:473-8
5. Huang D, Camacho CV, Setlem R, Ryu KW, Parameswaran B, Gupta RK*, et al.* Functional interplay between histone H2B ADP-ribosylation and phosphorylation controls adipogenesis. Mol Cell **2020**;79:934-49 e14
6. Jayaram H, Hoelper D, Jain SU, Cantone N, Lundgren SM, Poy F*, et al.* S-adenosyl methionine is necessary for inhibition of the methyltransferase G9a by the lysine 9 to methionine mutation on histone H3. Proc Natl Acad Sci U S A **2016**;113:6182-7
7. Gupte R, Nandu T, Kraus WL. Nuclear ADP-ribosylation drives IFNgamma-dependent STAT1alpha enhancer formation in macrophages. Nat Commun **2021**;12:3931
8. Lin KY, Huang D, Kraus WL. Generating protein-linked and protein-free mono-, oligo-, and poly(ADP-ribose) in vitro. Methods Mol Biol **2018**;1813:91-108
9. Zhang T, Berrocal JG, Yao J, DuMond ME, Krishnakumar R, Ruhl DD*, et al.* Regulation of poly(ADP-ribose) polymerase-1-dependent gene expression through promoter-directed recruitment of a nuclear NAD+ synthase. J Biol Chem **2012**;287:12405-16
10. Zhong S, Joung JG, Zheng Y, Chen YR, Liu B, Shao Y*, et al.* High-throughput illumina strand-specific RNA sequencing library preparation. Cold Spring Harb Protoc **2011**;2011:940-9
11. Kim D, Pertea G, Trapnell C, Pimentel H, Kelley R, Salzberg SL. TopHat2: accurate alignment of transcriptomes in the presence of insertions, deletions and gene fusions. Genome Biol **2013**;14:R36
12. Wang L, Wang S, Li W. RSeQC: quality control of RNA-seq experiments. Bioinformatics **2012**;28:2184-5
13. Trapnell C, Williams BA, Pertea G, Mortazavi A, Kwan G, van Baren MJ*, et al.* Transcript assembly and quantification by RNA-Seq reveals unannotated transcripts and isoform switching during cell differentiation. Nat Biotechnol **2010**;28:511-5
14. Huang da W, Sherman BT, Lempicki RA. Systematic and integrative analysis of large gene lists using DAVID bioinformatics resources. Nat Protoc **2009**;4:44-57

15. Ramirez F, Ryan DP, Gruning B, Bhardwaj V, Kilpert F, Richter AS*, et al.* deepTools2: a next generation web server for deep-sequencing data analysis. Nucleic Acids Res **2016**;44:W160-5

16. Corces MR, Trevino AE, Hamilton EG, Greenside PG, Sinnott-Armstrong NA, Vesuna S*, et al.* An improved ATAC-seq protocol reduces background and enables interrogation of frozen tissues. Nat Methods **2017**;14:959-62

17. Li H, Durbin R. Fast and accurate short read alignment with Burrows-Wheeler transform. Bioinformatics **2009**;25:1754-60

18. Chae M, Danko CG, Kraus WL. groHMM: a computational tool for identifying unannotated and cell type-specific transcription units from global run-on sequencing data. BMC Bioinformatics **2015**;16:222

19. Zhang Y, Liu T, Meyer CA, Eeckhoute J, Johnson DS, Bernstein BE*, et al.* Model-based analysis of ChIP-Seq (MACS). Genome Biol **2008**;9:R137

20. Feng J, Liu T, Qin B, Zhang Y, Liu XS. Identifying ChIP-seq enrichment using MACS. Nat Protoc **2012**;7:1728-40

21. Love MI, Huber W, Anders S. Moderated estimation of fold change and dispersion for RNA-seq data with DESeq2. Genome Biol **2014**;15:550

22. Bentsen M, Goymann P, Schultheis H, Klee K, Petrova A, Wiegandt R*, et al.* ATAC-seq footprinting unravels kinetics of transcription factor binding during zygotic genome activation. Nat Commun **2020**;11:4267

23. Krishnakumar R, Gamble MJ, Frizzell KM, Berrocal JG, Kininis M, Kraus WL. Reciprocal binding of PARP-1 and histone H1 at promoters specifies transcriptional outcomes. Science **2008**;319:819-21

24. Krishnakumar R, Kraus WL. PARP-1 regulates chromatin structure and transcription through a KDM5B-dependent pathway. Mol Cell **2010**;39:736-49

25. Martire S, Gogate AA, Whitmill A, Tafessu A, Nguyen J, Teng YC*, et al.* Phosphorylation of histone H3.3 at serine 31 promotes p300 activity and enhancer acetylation. Nat Genet **2019**;51:941-6

26. Langmead B, Salzberg SL. Fast gapped-read alignment with Bowtie 2. Nat Methods **2012**;9:357-9

27. Quinlan AR, Hall IM. BEDTools: a flexible suite of utilities for comparing genomic features. Bioinformatics **2010**;26:841-2

28. Heinz S, Benner C, Spann N, Bertolino E, Lin YC, Laslo P*, et al.* Simple combinations of lineage-determining transcription factors prime cis-regulatory elements required for macrophage and B cell identities. Mol Cell **2010**;38:576-89